

Expectation and Confusion: Evidence and Theory*

HENG CHEN

University of Hong Kong

YICHENG LIU

University of Hong Kong

August 16, 2025

Abstract. In this paper, we characterize a forecasting model where forecasters cannot perfectly distinguish between the two persistent components (trends and cycles) in a dynamic setting. In this model, forecasters jointly update their beliefs about the two components: noisy information about one component is used to update beliefs about the other component. We present diagnostic empirical facts on forecasting behaviors and show that these facts are consistent with our model's predictions while contradicting those of existing models in the expectation formation literature. To validate our model, we exploit the Federal Reserve's 2012 adoption of explicit inflation targeting as a policy shock. Structural estimation reveals that this policy change altered the underlying data-generation process, and the corresponding changes in forecasting behavior indeed align with our model's predictions. Finally, we characterize how this rational confusion mechanism interacts with behavioral biases such as overconfidence and show that this interaction can address the well-known persistent forecast error puzzle in the literature.

Keywords. expectation formation, forecasting, overconfidence, inflation expectation, Survey of Professional Forecasters.

JEL Classification. D83, D84, E37

*Heng CHEN: hengchen@hku.hk; Yicheng LIU: yicheng61@connect.hku.hk. The paper was previously circulated as "Trend, Cycle and Expectation Formation."

1 Introduction

There is growing interest in understanding how forecasters form expectations and make predictions about macroeconomic variables. The literature on expectation formation primarily focuses on how forecasters predict variables following a single component stationary process, with fewer studies investigating how they handle trends and cycles in their expectation formation process. In this paper, we introduce a simple framework to characterize how forecasters update their beliefs, form expectations, and make forecasts when macroeconomic variables contain trend components that cannot be perfectly distinguished from cyclical components.

Our first contribution in this paper is to provide empirical evidence on how forecasting behaviors vary across different forecast horizons—evidence that contradicts the aforementioned assumptions commonly used in existing models.

Second, we fully characterize a scenario where two persistent components (trends and cycles) cannot be perfectly disentangled in a dynamic setting. Our framework allows both the trend and cyclical components to be unobservable while also permitting both components to be persistent. This creates a more realistic and novel trend-cycle confusion mechanism that can account for the empirical patterns we document.

Third, we demonstrate how this rational confusion mechanism can interact with behavioral biases to generate new insights addressing empirical puzzles in the expectation formation literature, such as the persistent forecast error puzzle.

We begin our empirical analysis using the Survey of Professional Forecasters (SPF), which collects individual-level forecasts for macroeconomic variables at both short and long horizons.¹ First, we examine the covariance between changes in long-run and short-run cyclical forecasts at the forecaster level. We focus on this empirical moment because it maps directly to theoretical predictions and helps distinguish between competing models.

Specifically, we consider three-year-ahead forecasts for macroeconomic variables, such as the real GDP growth rate and the unemployment rate, as long-run forecasts. The difference between the h -quarters ahead forecast of a relevant macroeconomic variable and its three-year-ahead forecast is defined as the cyclical forecast, capturing short-run deviations from the long-run forecast. We then construct 'across-period changes' in both long-run and cyclical forecasts for each forecaster. Changes in long-run forecasts are calculated as the difference between their three-year-ahead forecasts in quarters t and $t - 1$. Similarly, we calculate changes in cyclical forecasts. By construction, changes in long-run forecasts reflect belief changes in both the trend and cyclical components, while changes in cyclical forecasts are proportional to belief changes

¹The SPF offers key advantages over alternative datasets: Blue Chip forecasts are limited to six quarters ahead without long-run projections, while Consensus Economics only provides long-run forecasts at the consensus level.

in the cyclical component.

Models that assume either an observable trend or a transitory cyclical component predict a non-negative covariance between changes in long-run forecasts and cyclical forecasts, as the same cyclical component drives both forecasters update their beliefs regarding the two components independently. Furthermore, these models predict that this covariance should decrease as h increases, converging to zero when h approaches three years, since the cyclical component plays a diminishing role over longer horizons.

However, our empirical findings contradict these theoretical predictions. For both real GDP growth and the unemployment rate, the covariance of interest is negative and increases as h increases in the SPF data. In other words, not only is the sign of the covariance opposite to what existing models predict, but its pattern over the forecast horizon h is also reversed.

Second, we examine how the cross-sectional dispersion of forecasts varies over the forecast horizon. Models that assume either an observable trend or a transitory cyclical component predict that forecast dispersion among forecasters should monotonically decrease as the forecast horizon increases. This is because disagreement among forecasters, caused by heterogeneous information about cyclical components, would diminish as the forecast horizon extends.²

Using the SPF data, we observe that for most macroeconomic variables (after being transformed into growth rates), forecast dispersion increases as the forecast horizon extends from zero to four quarters ahead. Additionally, we examine year-level forecast dispersion for real GDP growth and the unemployment rate over a longer forecast horizon and show that it increases as the horizon expands from one to three years. Interestingly, for inflation expectations, one of the most important macroeconomic variables, forecast dispersion decreases over horizons. These findings present a challenge for existing models and raise the question of how to reconcile both patterns of increasing and decreasing forecast dispersion across different variables and time horizons within one coherent framework.

Motivated by these findings, we propose an otherwise standard forecasting model that explicitly incorporates a non-stationary, unobservable trend component in the data generation process. Specifically, in this model, the state variable consists of a non-stationary random walk trend component and a cyclical component that follows the standard AR(1) process. The goal of forecasters is to minimize the squared error of their forecasts. The actual value of the state, which is the sum of these two components, is publicly announced and observed by forecasters at the end of each period.

²For example, if the forecasted variable is assumed to follow a stationary data generation process (e.g., an AR(1) process with a constant long-run mean), when the forecast horizon is long enough, all forecasts should converge to that long-run mean, and the forecast dispersion would approach zero.

The key assumption is that forecasters cannot directly observe the actual realizations of the trend and cyclical components. Instead, in each period, they receive two private noisy signals on the trend and cyclical components, respectively. This means that they are unable to differentiate the two components perfectly and must make inferences about them based on imperfect information.

In such a setting, forecasters need to update their beliefs about the trend and cyclical components *twice* in each period. At the beginning of each period, forecasters receive private signals regarding the trend and cyclical components and then revise their beliefs on each component. Forecasters use this set of posterior beliefs to make forecasts that minimize the expected forecasting errors. At the end of each period, the actual state value is disclosed, which is informative about both the trend and cyclical components. Consequently, forecasters must update their beliefs again, making revisions to their beliefs about the two components.

In this model, forecasters do not update their beliefs about the trend and cyclical components independently. In other words, they are rationally confused. Specifically, in the presence of this confusion mechanism, a strong signal about the cyclical component creates a positive surprise, which plays a dual role. First, it provides information about the cyclical component; therefore, forecasters revise their posterior beliefs regarding the cyclical component upwards from the prior beliefs inherited from the previous period. This is the standard belief updating mechanism. Second, such a positive surprise about the cyclical component is also useful for updating beliefs about the trend component. Forecasters rationally interpret the positive surprise as indicating they likely underestimated the cyclical component previously. Consequently, they would conclude that they had likely overestimated the trend component and would revise their current beliefs regarding the trend component downward.

In summary, the confusion between trend and cyclical components leads forecasters to rationally update their beliefs about these components in opposite directions. This mechanism gives rise to a negative covariance between the two beliefs. In the data, the constructed covariance between changes in long-term forecasts and changes in cyclical forecasts is proportional to the sum of the negative covariance of beliefs and the variance of beliefs about the cyclical component. When the confusion mechanism dominates, the covariance between changes in long-term and cyclical forecasts can be negative. Furthermore, as the forecast horizon h used to construct the cyclical forecasts increases, the constructed change in cyclical forecasts reflects a smaller proportion of the changes in cyclical components. Therefore, the covariance of changes in forecasts should also diminish in magnitude as h increases.

This mechanism can also account for the observed increase in forecast dispersion over horizons. In this model, for any forecast horizon, the dispersion of forecasts can be broken down into three parts: the dispersion caused by heterogeneous beliefs

about the cyclical component, the dispersion caused by heterogeneous beliefs about the trend component, and the covariance between these beliefs. The first part, the dispersion caused by heterogeneous beliefs about the cyclical component, always decreases over the forecast horizon, as the cyclical component becomes less influential for longer-term forecasts. The second part, the dispersion caused by heterogeneous beliefs about the trend component, remains constant over the forecast horizon, as the trend component is equally important for all horizons.

The third part, characterized by the *negative covariance* of cross-forecaster mean beliefs regarding the two components, is a novel aspect of the model. It stems from forecasters' use of signals regarding one component to update their beliefs about the other component. Furthermore, its importance diminishes over the forecast horizon as the cyclical component itself becomes less influential in forecasting. Therefore, the overall forecast dispersion could either increase or decrease over horizons. We show that forecast dispersion increases under the condition that the trend is neither too volatile nor too stable.

A few comments on our model are in order. First, we choose to model this rational confusion mechanism in a trend-cycle framework because we address specific empirical patterns and use data to validate our model mechanism. In fact, the confusion mechanism can be generalized to situations where both components are persistent without requiring a random walk component. Second, in existing models, forecasters would update their beliefs about the two components independently. This is either because forecasters could observe and therefore differentiate trends and cycles perfectly, or because of the cyclical component's lack of persistence. Finally, the key to our model is that forecasters must update their beliefs about the two components jointly even though they know these are two independent processes. This leads to the negative covariance between the two beliefs, which creates qualitative differences from existing models.

Model Validation: Explicit Inflation Targeting. Our model generates distinct forecasting patterns that vary with the underlying parameter space. Specifically, depending on the data-generating process, our model predicts that the covariance between changes in long-run and cyclical forecasts can be either positive or negative, while forecast dispersion may either increase or decrease across horizons. To validate these theoretical predictions, we exploit a policy shock that altered the data-generation process. By analyzing whether the subsequent changes in forecasting behavior align with our model's predictions, we can assess the validity of our proposed mechanism. Specifically, we examine the impact of implementing an inflation targeting policy in 2012 on forecasting behaviors. We demonstrate that the observed changes in forecasting behaviors following this policy shift are consistent with the predictions of our model, lending support to our proposed mechanism.

Rational Confusion and Behavioral Bias: Persistent Forecast Errors. We also extend our model to incorporate behavioral biases, which have been shown to be prevalent in the expectation formation process. The interaction between these biases and the rational confusion mechanism leads to qualitatively different model predictions compared to models lacking either feature, yet these predictions remain empirically relevant. Specifically, by introducing forecaster overconfidence in new information, our enhanced model addresses an important empirical puzzle: the positive correlation between consecutive forecast errors in SPF data, indicating that errors persist across periods rather than being serially independent (Ma et al. 2020).³ This persistent pattern cannot be rationalized by standard noisy information models with overconfidence, nor by our rational confusion mechanism alone. Rather, it emerges specifically from the interaction between these two mechanisms.

Discussion. In our benchmark model, we deliberately maintain a simple information structure to emphasize our novel core mechanism. We then extend our analysis to explore two alternative settings. First, we expand the model to allow forecasters access to a full range of multi-horizon forecasts from other forecasters at each period’s end. These forecasts provide information about aggregate beliefs on trend and cyclical components, enriching the forecasters’ information set. Despite this additional information, we show that forecasters still cannot perfectly differentiate between trend and cyclical components. While they can derive consensus forecasts for both components, these consensus forecasts retain time-varying errors. Importantly, our key qualitative results remain robust in this extended scenario.

We also examine an alternative scenario where confusion arises from forecasters misinterpreting signals. In such a model, forecasters observe trend and cyclical components at period-end but infer these components for the next period based on signals. Some forecasters may mistake trend signals for cyclical ones, and vice versa. This model can predict increasing forecast dispersion over horizons when the fraction of misinterpreting forecasters is moderate. However, it always predicts a non-negative covariance between changes in trend and cyclical forecasts, contradicting our findings.

Literature Review. This paper contributes to the literature on expectation formation in particular and information friction in general. First, it complements recent studies that use survey data to investigate expectation formation. Studies within the noisy information paradigm have found that forecasters tend to under-react to new information at the aggregate level (Coibion and Gorodnichenko 2015), but exhibit overreactions at the individual level (Bordalo et al. 2020; Angeletos and Huo (2021); Broer and Kohlhas 2024; Huo et al. 2024).⁴

³Ma et al. (2020) document that managerial forecast errors are positively and significantly autocorrelated, using the managerial survey from the Bank of Italy. We show that this puzzling fact also manifests in SPF data.

⁴New contributions to this literature further expand its scope. For instance, Kohlhas and Walther

A distinguishing feature of our work is that, unlike these studies which typically assume a stationary data-generating process for the state (often an AR(1) process), we examine scenarios incorporating a non-stationary trend component. This exploration is not only realistic but also empirically relevant, as prior research has established the presence of non-stationary trends in various macroeconomic variables, such as GDP growth rate (Stock and Watson 1998) and the unemployment rate (Blanchard and Summers 1986).⁵ Our work emphasizes that the unobservability of trends to forecasters is crucial for understanding the patterns of forecasting behaviors. This framework, even in its simplest form, yields several predictions that align with a set of empirical facts concerning how forecast behaviors vary over the forecast horizon.

Second, our model contributes to the existing literature on signal extraction problems in macroeconomics. Existing works focus on cases where forecasters cannot distinguish between persistent and transitory components (Muth 1960; Lucas and Prescott 1978; Collard et al. 2009; Lorenzoni 2009; Bostancı and Ordoñez 2024). Xie (2023) develops a Bayesian learning model of inflation expectations with time-varying parameters and noisy signals, highlighting the difficulty individuals face in separating structural shifts from noise. While her focus is on household expectations, the core idea, imperfect inference under persistent uncertainty, relates to our trend-cycle confusion mechanism. Our model differs in that, in a noisy information framework, forecasters need to separate two persistent components in a dynamic setting, which generates negatively correlated belief updates between the components. This is the key to accounting for forecasting patterns across forecasting horizons in our model.⁶

Third, our paper presents an evidence-motivated theoretical model, which is related to but distinct from previous quantitative works that utilize the trend-cycle framework. Farmer et al. (2024) presents a Bayesian learning model within a trend-cycle framework, focusing on model uncertainty about the data-generation process as a key friction rather than noisy information. Their model focuses on a representative forecaster and addresses several anomalies in consensus forecasts. In contrast, our work is grounded in the paradigm of noisy information and examines heterogeneity in individual forecasting behaviors, using variations in forecasting patterns across different horizons to inform the process of expectation formation. For example, our model can predict various patterns of cross-forecaster dispersion over different horizons.

(2021) explore why individual forecast errors are negatively correlated with current realizations, while Rozsypal and Schlaefmann (2023) examine how forecaster characteristics influence individual forecast errors. Chen et al. (2024) study individuals' heterogeneous overreaction to shocks of various properties.

⁵Early studies such as Nelson and Plosser (1982) and Harvey (1985) have demonstrated the presence of a non-stationary trend component in GDP growth. Similar findings have also been observed in studies analyzing inflation data, such as Cogley and Sargent (2005) and Cogley and Sbordone (2008).

⁶In this paper, we model a scenario where forecasters update their predictions for each macroeconomic variable individually. Wang and Hou (2024) presents empirical evidence supporting the realism of this forecasting behavior.

Fisher et al. (2025) study a behavioral model within a trend-cycle framework to address two important anomalies in long-run inflation expectation data: the persistent deviations of average expectations from actual trend inflation, and large and persistent disagreement regarding long-run inflation. In contrast, our key confusion mechanism is fully rational, and our work addresses a different set of empirical facts that apply to macroeconomic variables in general.

Finally, our work addresses the documented phenomenon that forecast dispersion tends to be larger in the long run. In the previous literature, studies have explained this pattern through either behavioral biases (Lahiri and Sheng 2008 and Patton and Timmermann 2010) or sticky information frameworks (Andrade et al. 2016). Our model offers a novel alternative, as the confusion mechanism we propose is fully rational rather than behavioral. Furthermore, a key distinctive prediction of our framework is that changes in trend forecasts and changes in cyclical forecasts can be negatively correlated – a feature that provides a clear empirical test to differentiate our approach from existing explanations.

2 Evidence

This section presents two key empirical findings from the U.S. Survey of Professional Forecasters (SPF). First, we document a negative covariance between changes in forecasters' long-term and cyclical forecasts. Second, we show that forecast dispersion among forecasters tends to increase with the forecast horizon for most macroeconomic variables.

2.1 Survey of Professional Forecasters Data

The Survey of Professional Forecasters (SPF) of the U.S. is a source of predictions made by professional forecasters regarding a broad range of macroeconomic variables. The data is collected quarterly and goes back to 1968Q4. The Fed of Philadelphia surveys approximately 35 professional forecasters each quarter, assigning a unique ID number to each forecaster to track their forecast history.

For each variable, a forecaster provides six predictions, including one back-cast toward the previous period, a now-cast (forecast for the current quarter), and forecasts for the subsequent four quarters. In addition, they are asked to provide The annual projection of this variable for the current year, and the next year. Since 1991Q4, the survey has included an extra question regarding the Consumer Price Index (CPI) for a ten-year forecast. Since 1992Q1, the first quarter survey has included an additional question about the GDP for a ten-year forecast, while since 1996Q3, the third quarter survey has incorporated an additional question regarding the natural unemployment rate. Starting from 2009, SPF has expanded to encompass year-level forecasts of the unemployment rate and real GDP for two- and three-year periods. Table A.1 in Ap-

pendix provides a summary of the starting dates and frequency for each data series.

The survey is conducted before the end of each quarter, following the Bureau of Economic Analysis' (BEA) advance report of the national income and product accounts (NIPA) release. The BEA reports macroeconomic variables (e.g., GDP estimates) for the preceding quarter. At the beginning of the questionnaire, forecasters will be provided with the BEA reported value of the macro variable for the previous quarter. Therefore, when giving their predictions for current and future quarters, forecasters have access to information about the values of forecasted variables up to the last quarter.

In Appendix A.4, we use the European Central Bank's Survey of Professional Forecasts (ECB-SPF) as a robustness check. The ECB-SPF provides individual forecasts for unemployment, real GDP growth, and inflation at multiple horizons: current year, next year, two years ahead, and long-run. This comprehensive horizon coverage enables us to proxy individual cyclical beliefs quarterly. Both the US-SPF and ECB-SPF have advantages over alternative datasets: Blue Chip forecasts are limited to six quarters ahead and lack long-run projections (except for inflation)⁷, and Consensus Economics only reports long-run forecasts at the aggregate level.

2.2 Covariance: Changes in Long Term Forecasts and Cyclical Forecasts

Building on this dataset, the following section presents a novel empirical test that examines the covariance between changes in forecasters' long-term and cyclical forecasts across time. We will show that the covariance of these changes is informative about the process of expectation formation.

We start our investigation by constructing forecasters' long-run forecasts and cyclical forecasts. As discussed earlier, since 2009, the Survey of Professional Forecasters (SPF) has asked forecasters each quarter to report their long term forecasts for the unemployment rate and real GDP, precisely three years ahead. We employ forecaster i 's three-year ahead forecast at quarter t , denoted as $F_{i,t}y_{t+3Y}$, to represent her long-run forecasts.⁸ Furthermore, we utilize the deviation of forecaster i 's forecast h period ahead at quarter t , denoted as $F_{i,t}y_{t+h}$, from the three-year ahead forecast as her cyclical forecast.

⁷While Blue Chip derives inflation expectations from various indicators ranging from 3-month T-bills to 30-year T-bonds, the spread between these rates cannot be interpreted as cyclical beliefs.

⁸A possible concern is that three-year-ahead forecasts may not adequately represent long-run forecasts. To address this, we utilize two forecast series with longer horizons: ten-year forecasts for real GDP (available every first quarter since 1992Q1) and forecasts of the natural unemployment rate (available every third quarter since 1996Q3). In Appendix A.2, we demonstrate that three-year-ahead forecasts are highly correlated with those for longer horizons, making them reasonable representations of long-run forecasts. We do not use the ten-year forecasts for GDP and the natural unemployment rate in our analysis due to the coarse frequency of observations at the yearly level. Instead, we focus on three-year-ahead forecasts, which are available at the quarterly level.

cal forecasts. Specifically, forecaster i 's cyclical forecasts is constructed as follows:

$$Cyc_{i,t}^h = F_{i,t}y_{t+h} - F_{i,t}y_{t+3Y}.$$

Then, we examine the covariance between the changes in the long-run forecasts and the cyclical forecasts:

$$COV_F^h = cov(F_{i,t}y_{t+3Y} - F_{i,t-1}y_{t-1+3Y}, Cyc_{i,t}^h - Cyc_{i,t-1}^h). \quad (1)$$

The first term on the right-hand side of Equation (1) represents the difference between three-year ahead forecasts for periods t and $t - 1$. The second term corresponds to the change in cyclical forecasts between these two periods. The horizon $h = 0, 1, 2, 3, 4$ represents the forecast horizon for the short-term forecast, which is utilized to construct the forecasts on cyclical components.

If the trend is perfectly observable to forecasters, this covariance shall be positive. This is because changes in cyclical forecasts reflect changes in the cyclical components from quarter t to quarter $t - 1$. Similarly, changes in long-term forecasts represent shifts in both the trend and cyclical components between these quarters. The covariance must be positive, provided that the innovations in trend and cyclical components are uncorrelated. Furthermore, the covariance should decrease as h (i.e., the forecast horizon for the short-term forecast used to construct cyclical forecast) increases, since the changes in cyclical forecasts would be less proportional to changes in cyclical innovations when h is longer.

If the cyclical component is not persistent (i.e., $\rho = 0$), this covariance should be zero. This is because changes in long-term forecasts would only represent shifts in the trend between these quarters. This set of predictions is characterized in Section 4.1.

Figure 2.1 illustrates the covariance between changes in long-run forecasts and cyclical forecasts for both the unemployment rate and real GDP growth. The x-axis represents the forecast horizons set at $h = 0, 1, 2, 3, 4$. Figure 1(a) shows the COV_F^h for the unemployment rate, while Figure 1(b) depicts the COV_F^h for real GDP growth. We observe a negative and significant COV_F^h for both variables, with the covariance increasing as the horizon h expands. Details of this estimation are shown in Table A.2.

These findings suggest that when a forecaster updates her long-run forecast upward, she tends to simultaneously revise her cyclical forecast downward. The empirical results reveal a pattern contrary to the predictions of the observable-trend model: not only is the covariance negative instead of positive, but it also increases over the horizon h rather than decreases.

In Appendix A.4, we present estimation results using ECB-SPF data for the unemployment rate, real GDP growth, and inflation. These results are consistent with

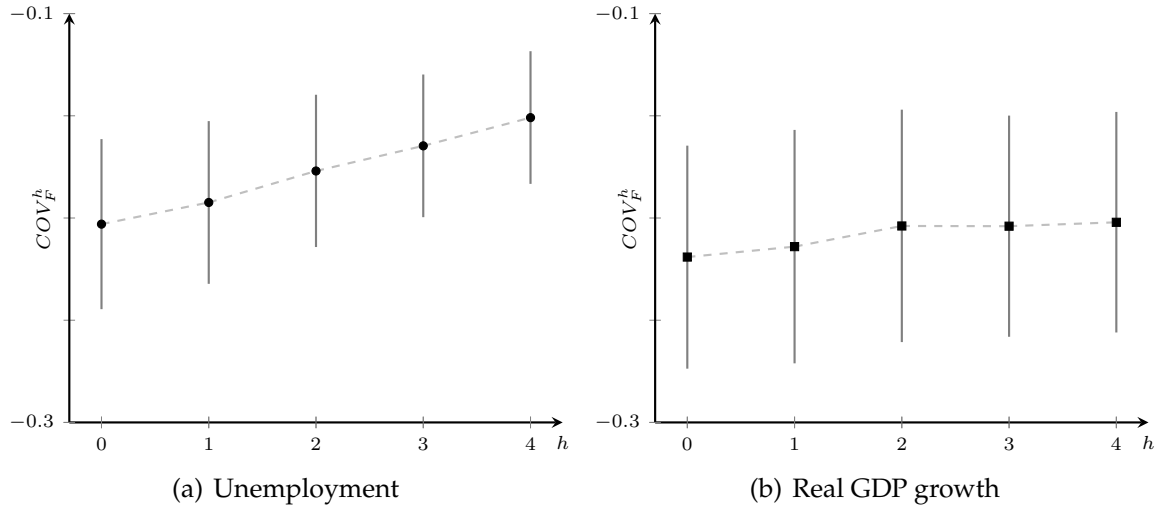


Figure 2.1. Covariance between the changes in long-run forecasts and cyclical forecasts across forecast horizon h . Note: This figure illustrates the covariance COV_F^h for the unemployment rate and real GDP growth across various forecast horizons h . The left panel shows the COV_F^h for the unemployment rate, while the right panel depicts the COV_F^h for real GDP growth. In both cases, the covariance is negative and statistically significant, increasing as the forecast horizon extends. The black dots represent the estimates, and the gray solid lines denote the 95% confidence intervals.

the pattern in Figure 2.1, where all three variables exhibit negative covariance that increases with the forecast horizon h .

2.3 Forecast Dispersion over Forecast Horizon

In this section, we explore whether the dispersion in forecasts among forecasters varies as the forecast horizon extends. This analysis provides insights into the role of beliefs concerning trends and cycles. If the trend is observable or the cyclical component lacks persistence, forecast dispersion should decrease monotonically as the forecast horizon increases, regardless of whether we examine short-term forecasts (within a year) or longer-term forecasts. This set of predictions will be characterized in Section 4.1.

First, we investigate the short-term forecasts, for which we have forecast data for most macroeconomic variables. Using SPF data, we estimate the following equation:

$$\text{Forecast dispersion}_{th} = \alpha + \beta_1 h + \epsilon_{th}, \quad (2)$$

where $\text{Forecast dispersion}_{th}$ represents the cross-forecaster dispersion in forecasts $F_{i,t}y_{t+h}$ provided by forecaster i at period t for h quarters ahead and the forecast horizon is defined as $h = 0, 1, 2, 3, 4$. The standard error is clustered at the year-quarter level.

We consider two measures of forecast dispersion: the variance of forecasts across forecasters and the difference between the 75th percentile and the 25th percentile. We estimate Equation (2) using all available macroeconomic variables. The estimated coefficient β_1 is of particular interest and is presented in Table 2.1.

Table 2.1. Forecast dispersion over forecast horizon

Forecast Variable	Dependent Variable: Forecast Dispersion				
	Variance of forecasts		50 percentile difference		Obs
	β_1	SE	β_1	SE	
(1)	(2)	(3)	(4)		
Nominal GDP	0.337***	0.026	0.204***	0.008	1,025
Real GDP	0.242***	0.022	0.162***	0.007	1,025
GDP price index inflation	0.118***	0.008	0.119***	0.004	1,025
Real consumption	0.125***	0.013	0.127***	0.006	770
Industrial production	0.860***	0.062	0.320***	0.014	1,025
Real nonresidential investment	1.647***	0.127	0.497***	0.018	770
Real residential investment	6.021***	0.547	0.932***	0.039	770
Real federal government consumption	1.284***	0.102	0.393***	0.019	770
Real state and local government consumption	0.317***	0.028	0.210***	0.009	770
Housing start	0.004***	0.000	0.020***	0.001	1,024
Unemployment	0.034***	0.002	0.081***	0.003	1,014
Inflation (CPI)	-0.066***	0.021	-0.073***	0.012	770
Three-month Treasury rate	0.091***	0.010	0.132***	0.007	770
Ten-year Treasury rate	0.045***	0.001	0.094***	0.003	560

Note: This table shows results from estimating Equation (2). The sample period is from 1968Q4 to 2019Q4. In column (1), the dependent variable is the variance of forecasts across forecasters. In column (3), we use the difference between the 25% percentile and 50% percentile. Standard errors are clustered at the year-quarter level.

Column (1) of Table 2.1 presents the results using forecast variance as the measure of forecast dispersion. The coefficient for the forecast horizon h is positive ($\beta_1 > 0$) and statistically significant for most variables, indicating that forecasts among forecasters become more dispersed as the forecast horizon increases. The only exception is inflation. We will revisit the analysis of inflation expectations in section 5. In column (3), we repeat our estimations using the difference between the 75th and 25th percentiles as the measure of forecast dispersion. The results are rather similar. To confirm that the pattern is robust to the inclusion of time fixed effect, we report the estimation results with year-quarter fixed effect in Table A.4. In addition, using the coefficient of variation as the measure of forecast dispersion, the results would be very similar.

Second, we investigate the longer-term forecasts, for which we have forecast data for fewer variables. Specifically, we focus on a subset of variables with annual forecast data that spans an extended horizon. Starting from 2009Q1, the U.S. Survey of Professional Forecasters (SPF) includes forecasts for real GDP and the unemployment rate one year, two years, and three years into the future. We utilize this dataset to estimate the following specification:

$$\text{Forecast dispersion}_{tH} = \alpha_2 + \sum_{H=1}^3 \beta_H \text{horizon}_H + \epsilon_t, \quad (3)$$

where $\text{Forecast dispersion}_{tH}$ is the dispersion of forecasts of horizon H across all forecasters and horizon_H is a dummy variable for horizon H , taking the value 1 if the

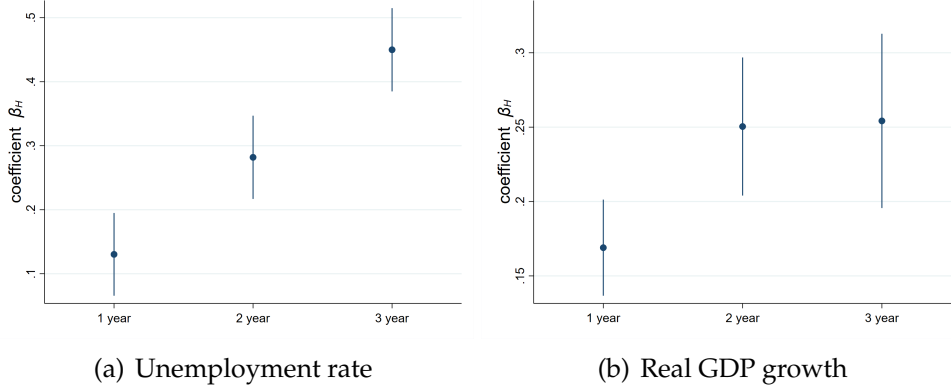


Figure 2.2. Dispersion of the year-level forecasts. Note: The figure presents the estimation results from Equation (3). The panel on the left displays the estimated coefficients for the unemployment rate, while the panel on the right shows those for real GDP growth. The sample period spans from 2009Q1 to 2019Q4. In both cases, β_H is greater than zero and increases as H increases, indicating larger dispersion as the forecast horizon expands.

forecast horizon is $H = 1$ year, 2 years, or 3 years ahead; and 0 otherwise. The coefficient β_H captures the difference in forecast dispersion between forecasts H years ahead and current year predictions ($H = 0$).

Figure 2.2 presents the estimation results. Figure 2(b) shows results for real GDP, while Figure 2(a) displays results for the unemployment rate. In both cases, the coefficients β_H are positive and increase with the forecast horizon. These findings also contradict the predictions of the observable-trend model, which states that dispersion should decrease monotonically.

In the literature, several studies have investigated this particular pattern, which offer similar findings that are inconsistent with the observable-trend model. Lahiri and Sheng (2008) use the *Consensus Forecasts* data and show that the forecast dispersion of real GDP growth is larger in a longer forecast horizon for all the G7 countries. Patton and Timmermann (2010) utilize the same data and find that both the forecast dispersion regarding the U.S. GDP growth and inflation is higher at longer horizons. Andrade et al. (2016) study the data from Blue Chip Survey and find a steady increase in the dispersion of Federal Fund rate forecasts as the forecast horizon extends.

3 Forecasting Model with Trend-cycle Confusion

3.1 Setup

Utility function. In this model, there exists a continuum of forecasters, indexed by $i \in [0, 1]$, who make forecasts about a stochastic state variable y_t . The objective of the forecasters is to minimize forecasting errors. We consider a standard quadratic utility

function, which is given by:

$$U(F_{i,t}y_{t+h}) = -(F_{i,t}y_{t+h} - y_{t+h})^2, \quad (4)$$

where y_{t+h} is the actual value of the state in period $t+h$ and $F_{i,t}y_{t+h}$ denotes the forecast made by forecaster i at period t for the state h periods in the future.

Data generation process. We assume that the state variable y_t is composed of two components: a trend component, μ_t , representing long-term trend, and a cyclical component, x_t , capturing short-term fluctuations. In particular, the trend follows a random walk process, while the cycle is modeled as an AR(1) process. Specifically, the data generation process for the state can be described as follows:

$$\begin{aligned} y_t &= \mu_t + x_t, \\ \mu_t &= \mu_{t-1} + \gamma_t^\mu, \\ x_t &= \rho x_{t-1} + \gamma_t^x, \end{aligned} \quad (5)$$

where ρ is the persistence for the AR(1) process and γ_t^μ and γ_t^x are the innovations of the trend and cyclical components, both of which are normally distributed with zero mean and variances of σ_μ^2 and σ_x^2 , respectively, i.e., $\gamma_t^\mu \sim N(0, \sigma_\mu^2)$ and $\gamma_t^x \sim N(0, \sigma_x^2)$. We use $\theta_t = (\mu_t, x_t)'$ to denote the state components in period t . Consistent with the previous literature, we assume that the data generating process (DGP) is common knowledge for all forecasters.⁹

In each period, forecasters receive private noisy signals for each component, that is, $s_{i,t} = (s_{i,t}^\mu, s_{i,t}^x)'$, where¹⁰

$$s_{i,t}^\mu = \mu_t + \epsilon_{i,t}; \quad \text{and} \quad s_{i,t}^x = x_t + e_{i,t}. \quad (6)$$

We assume that the error terms of the signals are independent and normally distributed. The variance-covariance matrix of i 's private signals is given by:

$$\Sigma_s = \begin{pmatrix} \sigma_\epsilon^2 & 0 \\ 0 & \sigma_e^2 \end{pmatrix}.$$

⁹In Appendix C.1, we discuss the scenario in which a common shock affects both the trend and cyclical components. This specification resembles that in Delle Monache et al. (2024). We demonstrate that this setting cannot produce the observed empirical patterns if the trend component is observable.

¹⁰Trend signals, reflecting long-run economic shifts, include announcements of structural reforms (e.g., deregulation), demographic projections, technological breakthroughs (e.g., AI advancements), changes to central bank inflation targets, and long-term policy framework adjustments. Conversely, cycle signals, indicating short-term fluctuations, include temporary supply chain disruptions, extreme weather events, fiscal stimulus measures (e.g., tax rebates), and inventory cycle updates. Forecasters also leverage proprietary research, such as business surveys and alternative data analysis, to be informed about both trend and cycle components.

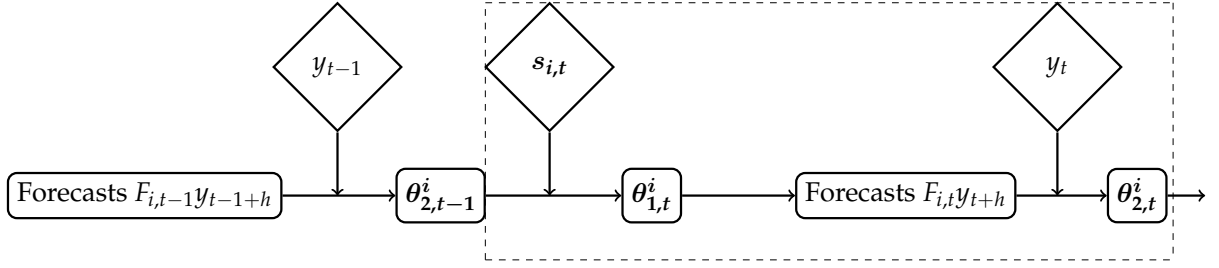


Figure 3.1. Timeline. In each period t , forecaster i will update her beliefs twice. First, based on the observed private signals, forecaster i adjusts her beliefs and provides forecasts for the current and future periods, i.e., $F_{i,t}y_{t+h}$. Second, forecaster i revises her beliefs regarding the trend and cyclical upon observing the actual realization of the state variable. The diamond boxes represent exogenous information flow. The squared boxes stands for the forecaster i 's beliefs.

At the end of each period t , we allow forecasters to observe the actual state variable y_t but not the trend and cyclical components. Therefore, upon the announcement of the actual state value, forecasters revise their beliefs regarding the trend and cyclical components. The updated beliefs about the two components become the prior beliefs for the next period.

Throughout the paper, we use $\theta_{1,t}^i$ to represent forecaster i 's posterior belief after forecaster i receive signals about the trend and cyclical components in period t (i.e., the first update). We use $\theta_{2,t}^i$ to represent forecaster i 's posterior belief after they observe the actual realization of the state in period t (i.e., the second update). The subscript 1 and 2 stand for the first and second updating in period t , respectively. We summarize the timeline of our setting in Figure 3.1:

- At the beginning of period t , forecaster i is endowed with the prior belief $\theta_{2,t-1}^i$, which is the posterior of the second updating from the period $t-1$.
- Forecaster i observes the private signal $s_{i,t}$ and then update her belief accordingly (the first updating).
- Given the updated beliefs $\theta_{1,t}^i$, forecasters choose their optimal forecasts of the current and future period $F_{i,t}y_{t+h}$.
- At the end of period t , y_t is revealed.
- Forecasters revise their beliefs again, forming beliefs $\theta_{2,t}^i$ (the second updating).

3.2 Equilibrium Characterization

In this section, we turn to the characterization of forecasters' optimal forecasts. We start our analysis by considering the posterior belief obtained from the second update in period $t-1$, which is the prior belief of forecaster i at the beginning of period t :

$$\theta_{2,t-1}^i = (\mu_{2,t-1}^i, \rho x_{2,t-1}^i)',$$

where $\mu_{2,t-1}^i$ and $x_{2,t-1}^i$ are forecaster i 's beliefs about trend and cyclical components at the end of period $t-1$, respectively. Let $z_{i,t-1}$ be forecaster i 's error in her belief regarding the trend in period $t-1$.

Lemma 1. Suppose the error term $z_{i,t-1}$ in period $t-1$ is normally distributed, then $z_{i,t}$ must also be normally distributed. The set of beliefs $\mu_{2,t-1}^i$ and $x_{2,t-1}^i$ can always be written in the form:

$$\mu_{2,t-1}^i \equiv \mu_{t-1} + z_{i,t-1} \quad \text{and} \quad x_{2,t-1}^i \equiv x_{t-1} - z_{i,t-1}, \quad (7)$$

which implies:

$$\mu_{2,t-1}^i + x_{2,t-1}^i = y_{t-1}.$$

The proof and subsequent proofs are collected in Appendix B. In the following, we call $z_{i,t-1}$ the *separation error*. First, if the separation error follows a normal distribution in one particular period, it will continue to be normally distributed indefinitely, given that both the state innovations and signals are also normally distributed. Second, given the actual y_{t-1} is observed at the end of $t-1$, the normality assumption and the Bayes' rule requires that beliefs regarding the two components $\mu_{2,t-1}^i$ and $x_{2,t-1}^i$ must sum up to y_{t-1} . That is, the error terms in the two beliefs are of the same magnitude but opposite in sign.

Denote the variance of $z_{i,t-1}$ as $\sigma_{z,t-1}^2$, then the variance-covariance matrix of $\theta_{2,t-1}^i$ follows:

$$\Sigma_{\theta_{2,t-1}^i} = \begin{pmatrix} \sigma_{z,t-1}^2 + \sigma_{\mu}^2 & -\rho\sigma_{z,t-1}^2 \\ -\rho\sigma_{z,t-1}^2 & \rho^2\sigma_{z,t-1}^2 + \sigma_x^2 \end{pmatrix}.$$

The sub-diagonal term $-\rho\sigma_{z,t-1}^2$ in the covariance matrix is negative. Intuitively, if a forecaster believes that the trend is stronger than it actually is (i.e., forecasting error on the trend component is positive), she will tend to believe that the cyclical component is weaker than it actually is, and vice versa. Note that when forecasters can perfectly distinguish between the trend and cyclical components, the corresponding sub-diagonal term will be zero. We will refer to $\sigma_{z,t}^2$ as the extent of confusion in distinguishing between the trend and cyclical components.

Lemma 2. There exists a unique steady state σ_z^2 for the variance $\sigma_{z,t}^2$.

The variance $\sigma_{z,t}^2$ always converges to a steady-state value, σ_z^2 . To understand why the variance of the error term, or the extent of confusion, converges, we observe two opposing forces resulting from the observation of actual data y_t . On the one hand, the change in state provides information about the cyclical component in the last period, given by $y_t - y_{t-1} = -(1 - \rho)x_{t-1} + \gamma_t^x + \gamma_t^{\mu}$. This assists forecasters in separating the cyclical component from the trend, reducing their confusion. On the other hand,

because y_t comprises both components, forecasters use the observation of the state and their beliefs about trends (i.e., $y_t - \mu_{1,t}^i$) to revise their beliefs regarding the cyclical component x_t , thereby increasing their confusion.

When $\sigma_{z,t-1}^2$ is large, it implies lower-quality prior beliefs and therefore a lower quality of $\mu_{1,t}^i$. Consequently, the second force becomes less important, and the first force dominates, leading to a smaller $\sigma_{z,t}^2$. Conversely, when $\sigma_{z,t-1}^2$ is small, the second force dominates, resulting in an increase in the extent of confusion. Therefore, the steady-state value of σ_z^2 always exists. Throughout the paper, we assume that the separation error z_i has converged to the steady state, given the results are qualitatively similar when the error term has not converged.

In the following, we present how forecasters update their beliefs and make forecasts by following the timeline of events. The first step involves characterizing the process of belief updating after forecasters receive their private signals regarding trends and cycles. In period t , after acquiring the private signals $s_{i,t}$, forecaster i updates her beliefs on the trend and cyclical components and form her beliefs $\theta_{1,t}^i$, which is joint-normally distributed. The expectations of these beliefs are given by:

$$\theta_{1,t}^i = \theta_{2,t-1}^i + \kappa \times (s_{i,t} - \theta_{2,t-1}^i), \quad (8)$$

where κ is the Kalman gain and $(s_{i,t} - \theta_{2,t-1}^i)$ is the surprise from signals:

$$\kappa = \begin{pmatrix} \frac{V + \sigma_e^2(\sigma_z^2 + \sigma_\mu^2)}{\Omega} & -\frac{\rho\sigma_e^2\sigma_z^2}{\Omega} \\ -\frac{\rho\sigma_e^2\sigma_z^2}{\Omega} & \frac{V + \sigma_e^2(\sigma_x^2 + \rho^2\sigma_z^2)}{\Omega} \end{pmatrix} \quad \text{and} \quad s_{i,t} - \theta_{2,t-1}^i = \begin{pmatrix} s_{i,t}^\mu - \mu_{2,t-1}^i \\ s_{i,t}^x - \rho x_{2,t-1}^i \end{pmatrix}.$$

The variance-covariance matrix of $\theta_{1,t}^i$ is given by:

$$(\Sigma_s^{-1} + \Sigma_{\theta_{2,t-1}^i}^{-1})^{-1} = \begin{pmatrix} \text{Var}^T & \widetilde{COV} \\ \widetilde{COV} & \text{Var}^C \end{pmatrix} = \begin{pmatrix} \frac{\sigma_e^2[\Omega - \sigma_e^2(\sigma_x^2 + \sigma_e^2 + \rho^2\sigma_z^2)]}{\Omega} & -\frac{\rho\sigma_e^2\sigma_z^2}{\Omega} \\ -\frac{\rho\sigma_e^2\sigma_z^2}{\Omega} & \frac{\sigma_e^2[\Omega - \sigma_e^2(\sigma_e^2 + \sigma_\mu^2 + \sigma_z^2)]}{\Omega} \end{pmatrix}, \quad (9)$$

where Ω and V are positive constants:

$$\Omega = (\sigma_z^2 + \sigma_\mu^2 + \sigma_e^2)(\sigma_x^2 + \sigma_e^2 + \rho^2\sigma_z^2) - \rho^2\sigma_z^4 \quad \text{and} \quad V = (\sigma_z^2 + \sigma_\mu^2)(\sigma_x^2 + \rho^2\sigma_z^2) - \rho^2\sigma_z^4.$$

The Kalman gain matrix κ has two parts. The elements on the main diagonal resemble those in the standard belief updating. That is, forecasters use signals about the trend (cycle) to update their beliefs on the trend (cycle).

When there is no confusion (i.e., σ_z^2 goes to zero), the model reduces to the standard Bayesian case. In this scenario, the Kalman gain for the trend component reduces

to $\sigma_\mu^2/(\sigma_\mu^2 + \sigma_e^2)$, and for the cyclical component, it reduces to $\sigma_x^2/(\sigma_x^2 + \sigma_e^2)$. When there is confusion (i.e., $\sigma_z^2 > 0$), the Kalman gain becomes larger than the Bayesian case without confusion. In other words, the confusion mechanism leads to less precise prior beliefs, and forecasters rely more on the signals, which provide new information. A similar argument holds true for the Kalman gain for the cyclical component.

Crucially, the non-zero elements on the sub-diagonal of the Kalman gain matrix, distinguish our model from the observable-trends model, where the counterpart terms are zero. This indicates that in our framework, forecasters incorporate information about the trend (cycle) component when updating their beliefs about the cyclical (trend) component. Consider a scenario where the private signal indicates that the cyclical component is stronger than the forecaster's prior belief. This situation could arise from three possibilities: Firstly, it might reflect a substantial positive innovation in the cyclical component itself. Secondly, it could be due to positive noise in the signal. Thirdly, it might suggest that the actual value of the cyclical component in the previous period was larger than what the forecaster believed. As forecasters cannot know the true value of each component with certainty, they will adjust their prior beliefs by increasing their estimate of the cyclical component from the last period and correspondingly decreasing their estimates of the trend component for both the last and current periods.

The variance-covariance matrix in Equation (9) warrants further discussion. Firstly, the elements on the main diagonal correspond to the perceived variance of the trend and cyclical components, which are influenced by the confusion mechanism. These variances are larger compared to the case where there is no confusion (i.e., the components can be perfectly observed). We denote them as Var^T and Var^C , respectively.

Secondly, the elements on the sub-diagonal components are non-zero and negative. That is, forecasters cannot perfectly distinguish between the trend and cycle, which gives rise to a negative covariance between the beliefs of these two components. Intuitively, when there are strong positive signals about the cyclical component, forecasters will simultaneously revise the cyclical component upward and the trend component downward. We denote this covariance of beliefs as $\widetilde{\text{COV}}$.

The second step is the stage of making forecasts. Forecaster i makes a series of forecasts about the state in h periods ahead. Under a quadratic utility function, her optimal prediction is the expected value of the state variable.

Lemma 3. The optimal forecast of forecaster i over horizon h is determined by their beliefs of trend and cyclical components, i.e.,

$$F_{i,t}y_{t+h} = E_{i,t}[\mu_t + \rho^h x_t] = \mu_{1,t}^i + \rho^h x_{1,t}^i.$$

This lemma says that the trend and cyclical beliefs play different roles over forecast

horizons: the trend belief consistently influences predictions across all horizons, while the influence of the cyclical belief diminishes as the forecast horizon extends.

The final step involves forecasters revising their beliefs again upon observing the actual value of the current state (y_t). This set of posterior beliefs becomes the prior beliefs for the next period. The forecasting error present in this set of posterior beliefs is the separation error ($z_{i,t}$). Lemma 4 characterizes its construction.

Lemma 4. Upon observing the actual state value y_t , the separation error $z_{i,t}$ present in the posterior beliefs is given by:

$$z_{i,t} = \frac{(\text{Var}^T + \widetilde{\text{COV}})(x_t - x_{1,t}^i) - (\text{Var}^C + \widetilde{\text{COV}})(\mu_t - \mu_{1,t}^i)}{(\text{Var}^T + \widetilde{\text{COV}}) + (\text{Var}^C + \widetilde{\text{COV}})}. \quad (10)$$

The extent of confusion σ_z^2 increases as σ_μ^2 , σ_x^2 , σ_e^2 , and σ_e^2 increase, converges to zero if any of these parameters goes to zero and is also bounded:

$$0 \leq \sigma_z^2 \leq \min\{\text{Var}^C, \text{Var}^T\}. \quad (11)$$

Recall that Var^T and Var^C represent the variances of forecasters' posterior beliefs regarding the trend and cyclical components, respectively, while $\widetilde{\text{COV}}$ denotes the corresponding covariance between the two components, as shown in Equation (9).

Lemma 4 states that the separation error after forecasters observe the actual state, is a weighted combination of the error terms in forecasters' beliefs regarding the trend and cyclical components *before* they observe the actual state. If they over-predict the trend component (i.e., $\mu_t - \mu_{1,t}^i < 0$), then $z_{i,t}$ tends to be positive. Conversely, if they over-predict the cyclical component (i.e., $x_t - x_{1,t}^i < 0$), then $z_{i,t}$ tends to be negative.¹¹

Note that after observing the actual state value, the covariance between beliefs regarding the trend and cyclical components is represented as $-\sigma_z^2$. The extent of confusion, denoted by σ_z^2 , is influenced by two primary factors: the quality of signals (i.e., σ_e^2 and σ_e^2) and the volatility of the state variables (i.e., σ_μ^2 and σ_x^2). First, forecasters receive private signals about each component in every period, which help them differentiate between the two. Consequently, more accurate signals decrease the level of confusion. Second, when the state innovations in the trend or cyclical component are more volatile, it becomes more difficult to identify each component, resulting in a higher level of confusion. Intuitively, the confusion is upper bounded by the uncertainty in either the trend or cyclical beliefs.

¹¹Consider a special case nested in Equation (10). When the trend is stable (i.e., $\sigma_\mu^2 = 0$), forecasters can predict the trend component perfectly. Therefore, the error term in their beliefs regarding the trend component is zero. In this scenario, both the variance of the belief regarding the trend component (Var^T) and the covariance ($\widetilde{\text{COV}}$) would also be zero. As a result, the separation error in this case would be zero.

4 Forecasts over Horizon: Main Results

4.1 Special Case: Independent Updating

Before presenting our model predictions regarding forecasting behaviors over the forecast horizon, we examine a special case where trends are stochastic, but forecasters can observe the actual trend component at the end of each period. This allows forecasters to perfectly distinguish between the trend and cyclical components. In this scenario, the key information friction in our model is absent (i.e., $\widetilde{COV} = 0$), while all other assumptions remain unchanged. The case where the cyclical component is transitory is analogous. Contrasting this special case and our benchmark model helps illustrate the importance of the information friction arising from trends and cycles not being separable.

In this case, forecasters can perfectly separate the two components, which implies that the separation error becomes zero (i.e., $z_{i,t} = 0$) and the variance of the separation error also reduces to zero (i.e., $\sigma_z^2 = 0$). Consequently, both the Kalman gain matrix in Equation (8) and the variance-covariance matrix in Equation (9) become standard:

$$\kappa = \begin{pmatrix} \frac{\sigma_\mu^2}{\sigma_\mu^2 + \sigma_\epsilon^2} & 0 \\ 0 & \frac{\sigma_x^2}{\sigma_x^2 + \sigma_\epsilon^2} \end{pmatrix} \quad \text{and} \quad \begin{pmatrix} \text{Var}_s^T & \widetilde{COV}_s \\ \widetilde{COV}_s & \text{Var}_s^C \end{pmatrix} = \begin{pmatrix} \frac{\sigma_\epsilon^2 \sigma_\mu^2}{\sigma_\epsilon^2 + \sigma_\mu^2} & 0 \\ 0 & \frac{\sigma_\epsilon^2 \sigma_x^2}{\sigma_x^2 + \sigma_\epsilon^2} \end{pmatrix}.$$

In this scenario, the sub-diagonal elements of the Kalman gain matrix are zero, indicating that forecasters do not use information from the trend or cyclical component to update their beliefs about the other. That is, they treat these components as independent, resulting in zero covariance (i.e., $\widetilde{COV}_s = 0$).

In the following, we investigate whether this model could help address the two empirical patterns documented in section 2. We first examine the covariance between changes in long-run forecasts and cyclical forecasts. Keep in mind that in the empirical analysis, we take three-year-ahead forecasts (i.e., $h = 3Y$) as forecasters' long-run forecasts. We calculate the difference between h -quarter-ahead forecasts and three-year-ahead forecasts to obtain the cyclical forecasts. We construct the exact model counterparts as follows:

$$F_{i,t}y_{t+3Y} - F_{i,t-1}y_{t-1+3Y} = (E_{i,t}[\mu_t] - E_{i,t-1}[\mu_{t-1}]) + \rho^{3Y}(E_{i,t}[x_t] - E_{i,t-1}[x_{t-1}]),$$

and

$$Cyc_{i,t}^h - Cyc_{i,t-1}^h = (\rho^h - \rho^{3Y})(E_{i,t}[x_t] - E_{i,t-1}[x_{t-1}]).$$

Therefore, the model predicts a positive covariance between changes in the long-run

forecasts and cyclical forecasts:

$$COV_F^h = \rho^{3Y}(\rho^h - \rho^{3Y})Var(E_{i,t}[x_t] - E_{i,t-1}[x_{t-1}]) > 0.$$

It holds because the belief updating of trend and cyclical components is independent (i.e., $\widetilde{COV}_s = 0$) and the covariance between the changes in trend beliefs and cyclical beliefs is zero, i.e., $cov(E_{i,t}[\mu_t] - E_{i,t-1}[\mu_{t-1}], E_{i,t}[x_t] - E_{i,t-1}[x_{t-1}]) = 0$. In addition, as the forecast horizon h increases, the model predicts that COV_F^h decreases with h , since ρ is less than one.

Furthermore, in this special case, the forecast variance across forecasters can be decomposed into two components:

$$\text{Forecast dispersion}_{th} = E[(F_{i,t}y_{t+h} - \bar{E}[F_{i,t}y_{t+h}])^2] = \rho^{2h}\phi_s^C \text{Var}_s^C + \phi_s^T \text{Var}_s^T, \quad (12)$$

where $\phi_s^C = \sigma_x^2/(\sigma_x^2 + \sigma_e^2) < 1$, $\phi_s^T = \sigma_\mu^2/(\sigma_\mu^2 + \sigma_e^2) < 1$ and $\bar{E}[\cdot]$ is the mean forecast across all forecasters. Note the dispersion of forecasts across forecasters is smaller than the variance of individual forecasters' beliefs because their information sets are correlated. This explains why both ϕ_s^C and ϕ_s^T are less than one.

When the forecast horizon h increases, the dispersion across forecasters caused by their noisy information on the cyclical component becomes less significant, i.e., ρ^{2h} decreases in h . However, the dispersion caused by their noisy information on the trend component remains stable over the horizon. As a result, the total dispersion decreases monotonically over the forecast horizon.

In summary, when trends and cycles are separable, the model fails to generate either of the two empirical patterns documented. In fact, its predictions are exactly opposite to the observed patterns in the data. We further extend this special case by allowing the data generation process to be a general ARMA model instead of an AR(1). However, this does not alter the model predictions. Further discussion of this result is provided in Appendix B. Moving forward, we will elaborate on the scenario where the two components are not perfectly separable. We will then explore the conditions under which the model predictions can be reversed.

4.2 Covariance of Beliefs

The key difference between our benchmark model and the special case is that forecasters jointly update their beliefs regarding the two components. As a result, their beliefs about these two components are correlated, even when they are, in fact, independent. In this section, we analyze the covariance between forecasters' beliefs regarding trends and cycles after they have observed their private signals.

The covariance between forecasters' beliefs about the trend and cyclical components, captured by \widetilde{COV} in Equation (9), is a crucial element of our model. This co-

variance depends on the volatility of the two components as well as the persistence of the cyclical component. Proposition 1 provides a detailed characterization of how these factors determine the sign and magnitude of the covariance of beliefs.

Proposition 1. *(i) The magnitude of the covariance between the trend and cyclical beliefs $|\widetilde{\text{COV}}|$ first increases and then decreases in the variance of trend innovations σ_μ^2 ; and it is zero when $\sigma_\mu^2 = 0$ and converges to zero when σ_μ^2 goes to ∞ . (ii) The magnitude of the covariance increases with the persistence of the cyclical component (ρ). In particular, when $\rho = 0$, $\widetilde{\text{COV}} = 0$.*

To understand part (i), recall the covariance is characterized by $\widetilde{\text{COV}} = -\rho\sigma_e^2\sigma_e^2\sigma_z^2/\Omega$. As the variance of trend innovations (σ_μ^2) increases, two effects emerge. Firstly, Lemma 4 has shown that forecaster i 's confusion, represented by σ_z^2 , increases. Secondly, forecaster i 's uncertainty about the state, represented by Ω , also increases. When the variance of trend innovations remains relatively small, the increase in confusion (σ_z^2) dominates. Conversely, when it is relatively large, the increase in overall variance (Ω) dominates.

Consider the following polar cases. When the trend is stable (i.e., $\sigma_\mu^2 = 0$), there is no confusion (i.e., $\sigma_z^2 = 0$). Therefore, the covariance is zero. When the trend innovation is very large (i.e., $\sigma_\mu^2 \rightarrow \infty$), forecaster i 's uncertainty about the state is also very large (i.e., $\Omega \rightarrow \infty$), the confusion mechanism becomes irrelevant, and the covariance converges to zero too.

To understand part (ii), we first examine an extreme case where the persistence of the cyclical component is zero (i.e., $\rho = 0$). That is, the cyclical component becomes purely transitory, and our model reduces to a standard signal extraction problem. Consequently, signals regarding the cyclical components offer information solely about the cyclical components, which are uninformative for the trend components. Therefore, the covariance of beliefs regarding the two components is rendered to be zero. As the persistence (ρ) of the cyclical component increases, signals regarding the cyclical components become more valuable for revising trend beliefs, giving rise to a larger covariance in magnitude.

4.3 Covariance between changes of long-run forecasts and cyclical forecasts

In this section, we examine the model's prediction for the covariance between changes in long-run and cyclical forecasts, which can be constructed from the data. Interestingly, we can relate the observable covariance in the data to the unobservable covariance between trend and cyclical beliefs in the model. We show the necessary and sufficient conditions under which our model can produce either a positive or negative covariance between changes in long-run and cyclical forecasts, and that the magnitude of the covariance decreases as the horizon h increases.

We begin our analysis by decomposing both the changes in the long-run forecasts and the cyclical forecasts. The changes in long-run forecasts is captured by changes in the forecasts for $h = 3Y$ periods ahead, which can be rewritten by:

$$F_{i,t}y_{t+3Y} - F_{i,t-1}y_{t-1+3Y} = (\mu_{1,t}^i - \mu_{1,t-1}^i) + \rho^{3Y}(x_{1,t}^i - x_{1,t-1}^i).$$

The changes in the long-run forecasts therefore reflect one's belief updates both in trend component (i.e., $\mu_{1,t}^i - \mu_{1,t-1}^i$) and cyclical component (i.e., $x_{1,t}^i - x_{1,t-1}^i$). On the other hand, the changes in the cyclical forecasts consist only the belief changes regarding the cyclical component:

$$Cyc_{i,t}^h - Cyc_{i,t-1}^h = (\rho^h - \rho^{3Y})(x_{1,t}^i - x_{1,t-1}^i). \quad (13)$$

The covariance between the changes in the long-run forecasts and cyclical forecasts can be written as follows:

$$\begin{aligned} & cov(F_{i,t}y_{t+3Y} - F_{i,t-1}y_{t-1+3Y}, Cyc_{i,t}^h - Cyc_{i,t-1}^h) \\ &= \underbrace{(\rho^h - \rho^{3Y})}_{(+)} \underbrace{\{\widetilde{COV} + \rho^{3Y} \text{Var}^C\}}_{(+)\text{ or }(-)}. \end{aligned} \quad (14)$$

The covariance COV_F^h can be positive or negative. For example, when a forecaster receives a signal indicating a stronger-than-expected cyclical component in the current period, she tends to revise the cyclical forecasts upwards. That is, $Cyc_{i,t}^h - Cyc_{i,t-1}^h > 0$. However, she can revise the long-term forecast either upwards ($F_{i,t}y_{t+3Y} - F_{i,t-1}y_{t-1+3Y} > 0$) or downwards ($F_{i,t}y_{t+3Y} - F_{i,t-1}y_{t-1+3Y} < 0$).

On the one hand, since the long-term forecast is partially driven by cyclical components, she may revise it upwards too. On the other hand, because the cyclical component is persistent, she revises her belief about the previous period's cyclical component upwards. This revision leads her to adjust her belief about the previous period's trend component downwards. This mechanism is shown in Section 3.2 (see Equation 9). It would suppress the estimate of trend component of the current period, causing a downward adjustment of the long-term forecasts.

The covariance term can be further decomposed into two parts, as shown in the second line of Equation (14). The first term, $(\rho^h - \rho^{3Y})$, is always positive and its magnitude depends on the forecast horizon h used to construct the cyclical forecasts. It decreases as the horizon h increases. When the cyclical forecast is constructed using the nowcast (i.e., $h = 0$), the first term reaches its largest value. As h approaches three years (i.e., $h = 3Y$), the first term goes to zero.

The second term can be either positive or negative. It consists of the covariance be-

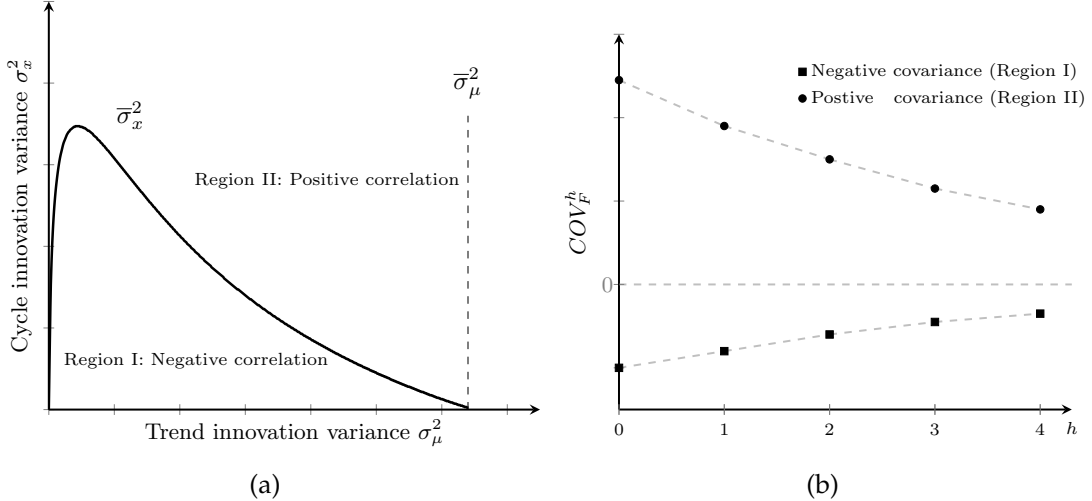


Figure 4.1. The sign and the magnitude of the covariance between changes in the long-run forecasts and cyclical forecasts. Figure 1(a) demonstrates the sign of the COV_F^h . For a pair of state innovation $(\sigma_\mu^2, \sigma_x^2)$, the model predicts a negative covariance, if it lies inside Region I and a positive covariance if it lies in Region II. Figure 1(b) plots the COV_F^h at horizon $h = 0, 1, 2, 3, 4$. The figure shows that the magnitude of COV_F^h is always decreasing in h .

tween trend and cyclical beliefs (i.e., \widetilde{COV}), and the variance of the cyclical belief (i.e., Var^C), each corresponding to one of the two mechanisms discussed earlier. Proposition 2 presents the necessary and sufficient conditions for the sum of the two terms to be negative.

Proposition 2. *There exists a threshold $\bar{\sigma}_\mu^2$ for the variance of the trend component innovation, such that:*

- (i) *for any $\sigma_\mu^2 \in [\bar{\sigma}_\mu^2, +\infty)$, COV_F^h is positive;*
- (ii) *for any $\sigma_\mu^2 \in (0, \bar{\sigma}_\mu^2)$, there exists a threshold $\bar{\sigma}_x^2$ such that COV_F^h is negative if and only if $\sigma_x^2 < \bar{\sigma}_x^2$; and it is positive, otherwise;*
- (iii) *and the magnitude of COV_F^h is decreasing as the horizon h increases.*

Figure 4.1 illustrates how the sign and the magnitude of COV_F^h change, which is characterized by Proposition 2. Figure 1(a) demonstrates the sign of COV_F^h as the variance of the trend and cyclical innovation varies. For a pair of signal quality (captured by σ_μ^2 and σ_x^2), the model predicts a negative covariance when the trend component is moderately volatile, and the cyclical component is not excessively volatile.

As shown in Equation (14), the changes in long-run forecasts and cyclical forecasts exhibit a negative covariance when \widetilde{COV} dominates. As shown in Proposition 1, this scenario occurs when the trend component is neither too stable nor too volatile. That explains item (i) in this proposition.

In addition, as the variance of the cyclical innovation (i.e., σ_x^2) increases, the variance of belief changes concerning the cyclical component (represented by the second

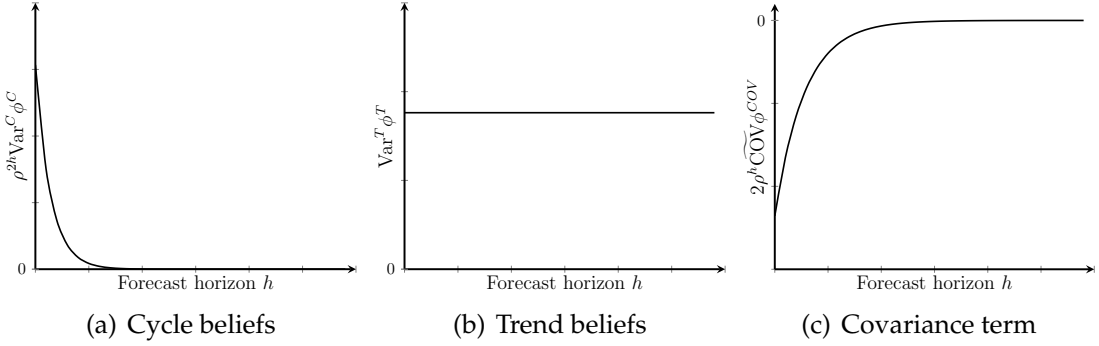


Figure 4.2. Dispersion decomposition as the horizon extends. Note: This figure shows how each part of the dispersion changes as the forecast horizon extends.

term on the right-hand side of Equation (14)) also increases. If the cyclical component is too volatile, the confusion mechanism becomes less relevant. We show the existence of a threshold, $\bar{\sigma}_x^2$, for the volatility of cyclical components, such that changes in trend forecasts and cyclical forecasts exhibit a negative covariance when σ_x^2 is lower than this threshold. This explains item (ii) in this proposition.

Figure 1(b) shows that the magnitude of COV_F^h decreases as the forecast horizon increases. As Equation (13) shows, as h increases, changes in cyclical forecasts correspond to a smaller proportion of cyclical updates. That is, $(\rho^h - \rho^{3Y})$ decreases in h . Therefore, the magnitude of the covariance decreases and converges to zero as the forecast horizon h increases. That explains item (iii) in this proposition.

4.4 Forecast dispersion

We proceed to examine the prediction of our model regarding the relationship between the forecast dispersion and the forecast horizon. In our model, the forecast dispersion can either increase or decrease as the forecast horizon becomes longer. Proposition 3 characterizes the necessary and sufficient conditions for the forecast dispersion to increase or decrease over the forecast horizon.

To expound the mechanism, we decompose the dispersion of forecasts across forecasters for any horizon into three components: the variance arising from heterogeneous beliefs about the trend component, the cyclical component, and their covariance. To be specific, the forecast dispersion is given by:

$$E[(F_{i,t}y_{t+h} - \bar{E}[F_{i,t}y_{t+h}])^2] = \rho^{2h} \text{Var}^C \phi^C + \text{Var}^T \phi^T + 2\rho^h \widetilde{\text{COV}} \phi^{\text{COV}}, \quad (15)$$

where $0 < \phi^C < 1$, $0 < \phi^T < 1$ and $0 < \phi^{\text{COV}} < 1$ are positive scalars, whose expressions are collected in the proof of Proposition 3. Note that $\bar{E}[\cdot]$ is the mean forecast across all forecasters.

Figure 4.2 illustrates how each part changes as the forecast horizon extends. Fig-

ure 2(a) shows that the variance from heterogeneous beliefs about the cyclical component decreases when the forecast horizon extends. This reduction occurs because the cyclical component's influence diminishes in longer-term forecasts. Figure 2(b) demonstrates that the variance due to heterogeneous beliefs about the trend component remains constant across all horizons. This is expected, as the trend component's influence is consistent regardless of the forecast horizon. The behavior of these two components over different horizons aligns with what is observed in the special case (see section 4.1).

Figure 2(c) depicts the covariance term. Its magnitude decreases as the forecast horizon extends, due to the diminished importance of the cyclical component over longer horizons. This feature, though intuitive, is crucial for understanding our model's predictions. On the one hand, the covariance term is negative, reducing overall forecast dispersion across forecasters for any horizon. On the other hand, as the forecast horizon extends, the impact of the covariance term diminishes, leading to a force that drives up the forecast dispersion.

The change in forecast dispersion over a longer horizon is determined by the relative strength of two forces: the diminishing force from dispersion due to heterogeneous beliefs about the cyclical component, and the increasing force from the covariance term. Interestingly, in this model, forecast dispersion must increase with the forecast horizon when h is large enough. The dispersion of cyclical beliefs converges to zero more rapidly as the forecast horizon extends than the covariance between trend and cyclical beliefs. This is evident from Equation (15): ρ^{2h} converges to zero more quickly than ρ^h . Therefore, when the forecast horizon is sufficiently long, the increasing force of the covariance becomes dominant, leading to greater dispersion. Proposition 3 fully characterizes this property.

Proposition 3. *The dispersion of forecasts across forecasters is strictly increasing in the forecast horizon h , if and only if:*

$$h > \underline{h} = \underbrace{\frac{1}{\ln \rho}}_{-} \underbrace{\ln \frac{-\widetilde{COV} \phi^{COV}}{Var^C}}_{- \quad or \quad +} W; \quad (16)$$

where $W < 1$ is a positive scalar given by $E[(z_{i,t} - E[z_{i,t}])^2] / \sigma_z^2$ and $\ln \rho < 0$.

When the threshold is negative ($\underline{h} \leq 0$), forecast dispersion always increases over the forecast horizon. This scenario occurs when the variance of the trend innovation is moderate. As shown in Proposition 1, in such cases, the impact of the covariance between trend and cyclical beliefs (i.e., \widetilde{COV}) is greatest.

Conversely, when the threshold value on the right-hand side of Equation (16) approaches infinity ($\underline{h} \rightarrow \infty$), forecast dispersion always decreases over the forecast hori-

zon. This scenario occurs in the special case described in section 4.1, where forecasters can perfectly differentiate between trend and cyclical components, resulting in a covariance term of zero.

5 Model Validation: Explicit Inflation Targeting

In the previous sections, we fully characterized our model and demonstrated how it generates various qualitative empirical patterns depending on the parameter space. Specifically, our model predicts that the covariance between changes in long-run forecasts and cyclical forecasts can be either positive or negative under certain conditions of the data generating process. Similarly, forecast dispersion can either increase or decrease over the forecast horizon depending on specific properties of the underlying processes.

To validate these theoretical predictions, we leverage a policy shock: a policy change that altered the underlying parameters of the data generating process. By examining whether the observed changes in forecasting patterns following this policy shift align with our model's predictions, we can assess the validity of our model mechanism.

Specifically, we examine the effects of the introduction of explicit inflation targeting in the United States in 2012. This new approach to monetary policy implementation began with an announcement on January 25th by Ben Bernanke, the Chairman of the U.S. Federal Reserve, who set a specific inflation target of 2%. Prior to this policy change, the United States did not have an explicit inflation target, relying instead on regularly announced desired target ranges for inflation.¹²

Through the lens of our model, the implication of this policy for forecasters is that the underlying data generation process for inflation could undergo changes which would necessitate changes in forecasting behaviors. To quantify the underlying changes caused by the policy implementation, we begin by dividing the sample into two sub-samples: the period before 2012 and the period after. We then structurally estimate the model using moments obtained from both the pre- and post-2012 sub-samples. We then assess the estimated changes in the data generation process and examine how they impact the empirical patterns of forecasts quantitatively. While all the details of the estimation are provided in Appendix A.6, we summarize the estimation procedures below. Note that we use the ten-year-ahead forecasts of the inflation rate in the SPF as the long-term forecasts because the SPF does not provide three-year-ahead forecasts for inflation. The ten-year-ahead forecast data have been available since 1991Q4.

¹²Before the era of the Greenspan Fed, the Federal Reserve operated under a stop-and-go policy without a specific inflation target. Starting in 1992, the Greenspan Fed aimed to maintain low long-term inflation rates (see Goodfriend 2004 for a comprehensive review). From the 1990s until the Great Recession, there was a consensus among market participants and FOMC members that the optimal inflation target would fall between 1% and 2%. However, there was no explicit inflation target (Shapiro and Wilson 2019). In January 2012, the FOMC announced a target of 2% for the inflation rate, marking the first time in its history that it adopted an explicit inflation-targeting approach.

Table 5.1. Estimated Model Parameters

Parameter Estimation						
	Pre-2012			Post-2012		
	Mean	90 HPDI	95 HPDI	Mean	90 HPDI	95 HPDI
σ_μ^2	1.14	(0.96,1.38)	(0.91,1.38)	0.84	(0.66,1.08)	(0.61,1.08)
σ_x^2	2.57	(2.41,2.67)	(2.43,2.75)	2.60	(2.37,2.76)	(2.40,2.88)
σ_ϵ^2	0.78	(0.62,0.89)	(0.61,0.95)	0.72	(0.48,0.89)	(0.47,0.97)
σ_e^2	1.62	(1.47,1.76)	(1.47,1.77)	1.54	(1.31,1.74)	(1.30,1.76)
ρ	0.84	(0.73,0.94)	(0.74,0.97)	0.64	(0.53,0.76)	(0.53,0.79)

Note: This table presents the estimated parameter values for the pre-2012 and post-2012 periods. We provide the mean values, as well as the 90% and 95% Highest Posterior Density Intervals (HPDI).

Our model can be fully specified by five parameters: $\{\rho, \sigma_\mu^2, \sigma_x^2, \sigma_\epsilon^2, \sigma_e^2\}$. The first three parameters are related to the data generating process, while the last two capture the precision of the signals. To structurally estimate the values of these parameters, we follow the approach of Chernozhukov and Hong (2003) and compute Laplace-type estimators (LTE) using a Markov Chain Monte Carlo method. To identify changes in the underlying parameters, we estimate them for each subsample period.

We estimated the model parameters by targeting the forecast variance across different horizons in each subsample period. We then used the estimated model to simulate data and examine the covariance patterns, which were not targeted in the estimation. This approach allowed us to assess the model's quantitative predictions about the effects of the policy shift in 2012.

To be concrete, we compute the across quarters average variances of forecasts for different horizons, specifically for $h = 0, 1, 2, 3, 4$, using the subsamples before and after 2012. These variances will be treated as the target moments in our estimation and denoted as \hat{m} . Furthermore, we construct the model counterpart of \hat{m} and define the distance between the two as follows:

$$\Lambda(\Theta) = [m(\Theta) - \hat{m}]' \hat{W} [m(\Theta) - \hat{m}], \quad (17)$$

where \hat{W} is the weighting matrix, where the diagonal elements represent the precision of the moments \hat{m} . We solve for the parameter values (Θ) to minimize the constructed distance, that is, finding the set of parameter values that best matches the forecast variance at each forecast horizon.

The estimated parameters for each subsample are reported in Table 5.1 together with the 90% and 95% high posterior density interval (HPDI). A comparison of the two sets of estimated parameters reveals that there are minimal changes in the innovations

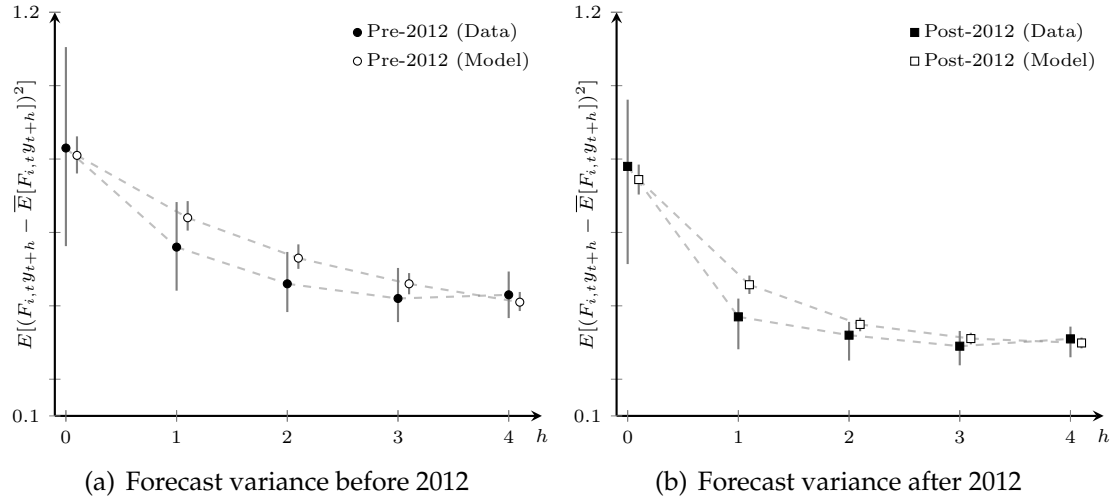


Figure 5.1. Forecast variance over horizon for the subsamples before and after 2012. Black dots represent results from SPF data, while white dots depict simulated data. Figure 1(a) shows forecast variance before 2012, and Figure 1(b) illustrates it after 2012. The gray solid line marks the 95% confidence interval using the bootstrap method. Our model fits the data closely in both sub-samples. The pre-2012 period spans from 1990Q1 to 2011Q4, and the post-2012 period from 2012Q1 to 2019Q4.

in cycles variance (i.e., σ_x^2) and the precision of signals on trends and cycles (i.e., σ_ϵ^2 and σ_ϵ^2) following the policy change in 2012. This indicates that this set of parameters remain relatively stable before and after the policy change.

There are two noteworthy changes. First, there is a sizable decrease in the variance of trend innovation (i.e., σ_μ^2). Before the policy change, the estimated variance was 1.14. After the policy change, it dropped to 0.84. This suggests that the trend is more stable after the policy implementation, consistent with the policy goal of providing a specific long-run target. Second, the persistence of the cyclical component (i.e., ρ) decreases. Before the policy change, the estimated persistence of the cyclical component was 0.84, aligning with previous literature. For instance, Carvalho et al. (2023) estimated a value of $\rho = 0.87$. After the policy change, the estimated persistence dropped to 0.64, indicating that short-term fluctuations have become less persistent. The observed change in the estimated persistence of the cyclical component is intuitive. Following the policy change, the central bank would respond more aggressively to short-term deviations from the long-term target. Consequently, the persistence of the cyclical component would decrease.

Next, we investigate whether the estimated model can reproduce the set of findings documented in Section 2 concerning inflation forecasts before and after 2012. First, we examine the forecast variance across various forecast horizons, which were targeted moments in the estimation. Figure 5.1 displays the forecast variance of the SPF data and the simulated data before and after 2012. The black dots represent results obtained using the SPF data, while the white dots represent the simulated data. The gray solid

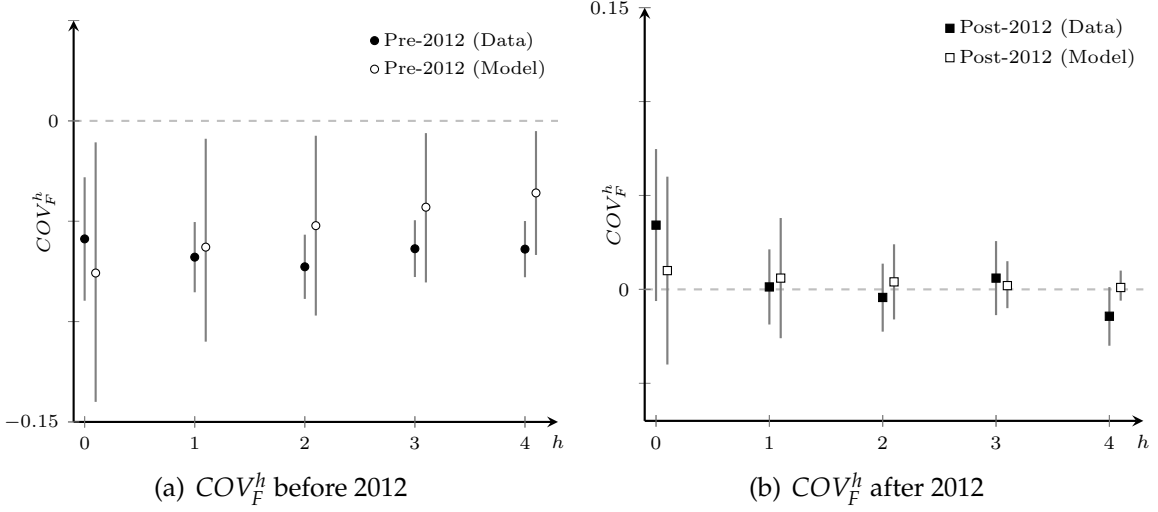


Figure 5.2. The estimated COV_F^h for the subsamples before and after 2012. Black dots represent the results obtained using SPF data, while white dots represent the simulated data. In Figures 2(a) and 2(b), we observe that the covariance is negative before 2012 and positive or close to zero after 2012. The sample period for the pre-2012 sub-sample ranges from 1990Q1 to 2011Q4, while the post-2012 sub-sample spans from 2012Q1 to 2019Q4.

line corresponds to the 95% confidence interval using the bootstrap method. In both sub-samples, the simulated models closely fit the empirical data.

In the SPF data, a notable difference between the two sample periods is observed: the forecast variance declines more rapidly as the forecast horizon extends in the post-2012 sub-sample compared to the pre-2012 period. Specifically, in the pre-2012 sub-sample, the forecast variance decreases by 32.5%, from 0.833 at the now-cast ($h = 0$) to 0.562 for forecasts one quarter ahead. In contrast, the post-2012 subsample exhibits a much sharper decline of 52.5%, with the variance dropping from 0.737 at the now-cast to 0.350 for one-quarter-ahead forecasts.

The change in empirical patterns across the two periods aligns qualitatively with our model's predictions. According to Proposition 1, when the trend component becomes more stable (i.e., σ_μ^2 decreases) and the cyclical component becomes less persistent (i.e., ρ decreases), the magnitude of the negative covariance between trend and cyclical beliefs decreases. This is because, as the trend component becomes more stable, forecasters can better separate the trend from the cycle; and as the persistence of the cyclical component decreases, new information about the cyclical component becomes less relevant for updating the trend component. As a result, the force from the confusion mechanism plays a less important role, and the overall forecast dispersion decreases at a faster rate.

Second, we examine the covariance between changes in the long-run forecasts and cyclical forecasts in both sub-samples. It is important to stress that this covariance was

not a targeted moment in the estimation.

The empirical results from the SPF data reveal an intriguing shift in forecasting behavior. Figure 2(a) shows a significant negative covariance between changes in long-run forecasts and cyclical forecasts in the pre-2012 sub-sample. In contrast, Figure 2(b) illustrates that this covariance becomes positive and insignificant in the post-2012 sub-sample.

This reversal in sign following the implementation of inflation targeting aligns with our model's prediction. As previously discussed, when the trend component becomes more stable and the cyclical component less persistent, the confusion mechanism's effect weakens. Consequently, the empirical covariance patterns should more closely match those predicted by the observable-trend model in section 4.1, where the confusion mechanism is absent. Our model predicts that after the policy change, the covariance between changes in trend forecasts and changes in cyclical forecasts is more likely to be non-negative.

Qualitatively, the estimated results from the simulated data closely align with the empirical results using the SPF data in both subsamples. Figure 5.2 contrasts the results in the SPF data with those from the simulation data. Despite its simplicity and limited number of parameters, our model effectively captures the shift in forecasting patterns following the policy change and quantitatively reproduces the changes observed in the actual data.

6 Rational Confusion and Behavioral Bias

In the previous sections, we show how the confusion mechanism plays a role by assuming that forecasters are rational and use the Bayesian rule to update their beliefs. In this section, we demonstrate that our framework can be extended to incorporate behavioral biases studied in the literature on expectation formation. We emphasize that the new confusion mechanism we introduce can interact with these biases and provide insights into various issues in the literature.

Specifically, we showcase this by introducing the feature of overconfidence, where forecasters subjectively believe that the variances of the signal noise are smaller than their actual values (e.g., Daniel et al. 1998 and Broer and Kohlhas 2024). We demonstrate how this extension of the benchmark model could address why now-cast errors might persist across periods, which is a well-known puzzle in the literature on expectation formation.

Following Ma et al. (2020), we examine the correlation between the now-cast errors across periods, using the SPF data. To be specific, we estimate the following equation:

$$\underbrace{y_t - F_{i,t}y_t}_{FE_{i,t}} = \alpha + \beta \underbrace{(y_{t-1} - F_{i,t-1}y_{t-1})}_{FE_{i,t-1}} + \epsilon_{i,t}, \quad (18)$$

Table 6.1. Forecast error persistence

Forecast Variable	Dependent Variable: Now-cast error		
	β	SE	Obs
	(1)	(2)	
Nominal GDP	0.154***	0.048	5,872
Real GDP	0.194***	0.057	5,907
GDP price index inflation	0.147**	0.064	5,803
Real consumption	-0.109*	0.064	4,122
Industrial production	0.303***	0.084	5,497
Real nonresidential investment	0.070	0.073	4,046
Real residential investment	0.120**	0.059	4,038
Real federal government consumption	-0.066	0.081	3,880
Real state and local government consumption	0.040	0.062	3,800
Housing start	0.261***	0.060	5,599
Unemployment	0.192***	0.056	5,489
Inflation (CPI)	0.044	0.065	4,188

Note: This table shows the coefficients obtained from estimating Equation (18). The sample period is from 1968Q4 to 2019Q4. Standard errors are clustered at the year-quarter level.

Table (6.1) displays the estimation results. In column (1), we observe that the estimated coefficient is significantly positive for the majority of macro variables. This suggests that the forecast error exhibits persistence over time: a larger (lower) now-cast error in the previous period is associated with a larger (lower) now-cast error in the current period.

This set of estimation results has two important implications. Firstly, in our benchmark model without behavioral bias, the estimated coefficients should be zero. It is straightforward that the now-cast error in the last period is already known to the forecasters when they provide their forecast in the current period. Therefore, the now-cast error across periods should be independent when the forecasters are fully rational. The significant estimated coefficients arising from this estimation indicate that forecasters deviate from the rational benchmark, highlighting the necessity of incorporating behavioral bias in our model.

Secondly, in a model where the confusion mechanism is absent and forecasters are overconfident, the now-cast errors across periods should still be zero. This is because the now-cast error in each period consists only of a weighted average of the state innovation and the signal noise. Overconfidence distorts the weights assigned to each component. However, both the innovations and signal noises are independent across periods; therefore, the correlation between now-cast errors across periods remains zero.

In the following, we investigate how the interplay between the two mechanisms – confusion and overconfidence – could account for this the documented empirical pattern. Specifically, to incorporate overconfidence, we consider a scenario where fore-

casters perceive the signal variances of the trend and cyclical components as $m_1\sigma_e^2$ and $m_2\sigma_e^2$ respectively. When $m_1 < 1$ ($m_2 < 1$), it indicates that forecasters subjectively believe the trend (cyclical) signal is more precise than it actually is.

Proposition 4. (i) *When forecasters are overconfident in the trend signal ($m_1 < 1$), the now-cast errors across periods are positively correlated if and only if*

$$\frac{\rho\sigma_e^2\sigma_\mu^2}{\sigma_e^2[\sigma_x^2 + (1-\rho)\sigma_e^2]} = \underline{m}_1 < m_1 < 1, \quad (19)$$

and negatively correlated otherwise. (ii) *When forecasters are overconfident in the cyclical signal ($m_2 < 1$), the now-cast errors across periods are positively correlated if and only if*

$$1 < \frac{1}{m_2} < \frac{1}{\underline{m}_2} = \frac{\sigma_e^2[\rho\sigma_\mu^2 - (1-\rho)\sigma_e^2]}{\sigma_e^2\sigma_x^2} \quad (20)$$

and negatively correlated otherwise.

To explicate the proposition, we observe that the now-cast error of period t consists of three parts: the state innovations of period t , the noise of the new signals, and the separation error inherited from the previous period ($z_{i,t-1}$). Since the state innovations and the noise in the private signals are independent across periods, the component of the now-cast error generated by the current state innovation and signal noise must be independent of the now-cast error from the previous period ($FE_{i,t-1}$). In other words, the correlation between the now-cast errors in the last period ($FE_{i,t-1}$) and the current period ($FE_{i,t}$) must be driven by their correlations with the separation error from the last period ($z_{i,t-1}$).

First, we analyze the correlation between the separation error from the previous period ($z_{i,t-1}$) and the now-cast error from that same period ($FE_{i,t-1}$). We show that the covariance between these two errors is given by:

$$cov(z_{i,t-1}, FE_{i,t-1}) = -(1-m_1)\sigma_e^2\sigma_e^2\phi_O^T \frac{V_1}{\Omega_1} \leq 0, \quad (21)$$

where ϕ_O^T is a positive scalar, and V_1 and Ω_1 are counterparts of V and Ω , respectively. Detailed expressions of these variables are provided in Appendix B.

In the Bayesian benchmark (i.e., $m_1 = 1$), as implied by Equation (21), the covariance would be zero. Intuitively, the forecast error $z_{i,t-1}$ must be orthogonal to any information already known to the forecasters ($FE_{i,t-1}$) under rational expectation.

When forecasters exhibit overconfidence in trend signals (i.e., $m_1 < 1$), Equation (21) dictates that the covariance is always negative. In such cases, forecasters' beliefs about trends rely more on the trend signal relative to the Bayesian benchmark. Therefore, both the separation error and their now-cast will move in the same direction,

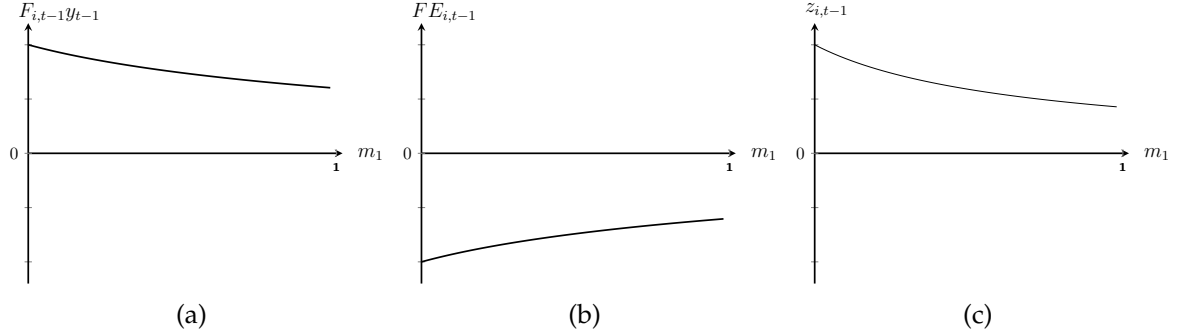


Figure 6.1. The now-cast, now-cast error and the separation error in period $t - 1$ under overconfidence. Note: The figure plots the now-cast, now-cast error, and separation error for period $t - 1$ at a given level of overconfidence $m_1 < 1$. When forecasters are overconfident, compared to the rational benchmark, last period's now-cast and separation error move in the same direction, while the now-cast error moves in the opposite direction.

while the now-cast error moves in the opposite direction.

To illustrate, consider a case where the trend signal contains a positive surprise in period $t - 1$. The overconfident forecaster would assign a higher weight to this surprise and overestimate the trend component. Consequently, the now-cast from period $t - 1$ (i.e., $F_{i,t-1}y_{t-1}$) exceeds what a Bayesian forecaster would predict. Therefore, the corresponding now-cast error, $FE_{i,t-1}$, which is the difference between now-cast and the realization y_{t-1} , is lower than the Bayesian benchmark. Similarly, the separation error, $z_{i,t-1}$, which is the difference between the trend belief after observing realization y_{t-1} , is also higher than in the rational case. As a result, the covariance between the separation error and the now-cast error from period $t - 1$ is no longer zero; it becomes negative.

Then, we turn to analyze how this separation error ($z_{i,t-1}$) affects the now-cast error in the current period ($FE_{i,t}$). When forecasters are overconfident in the trend signal, the covariance between the separation error and the now-cast error for the current period can be written as follows:

$$\text{cov}(z_{i,t-1}, FE_{i,t}) = \frac{\sigma_z^2}{\Omega_1} \underbrace{[-m_1 \sigma_e^2 (\sigma_x^2 + \sigma_e^2)]}_{\text{trend prior effect}} + \underbrace{\rho \sigma_e^2 (\sigma_\mu^2 + m_1 \sigma_e^2)}_{\text{cyclical prior effect}}. \quad (22)$$

Recall that the separation error inherited from period $t - 1$ is present in the prior belief for period t , and it exerts opposite effects on prior beliefs regarding trend and cyclical components (see Equation (7)). Specifically, if the separation error $z_{i,t-1}$ is positive, compared to the case without a separation error, the trend prior leads to a larger now-cast and a lower $FE_{i,t}$; whereas the cyclical prior leads to a smaller now-cast and a larger $FE_{i,t}$. That is why the effect of the trend prior is negative and the

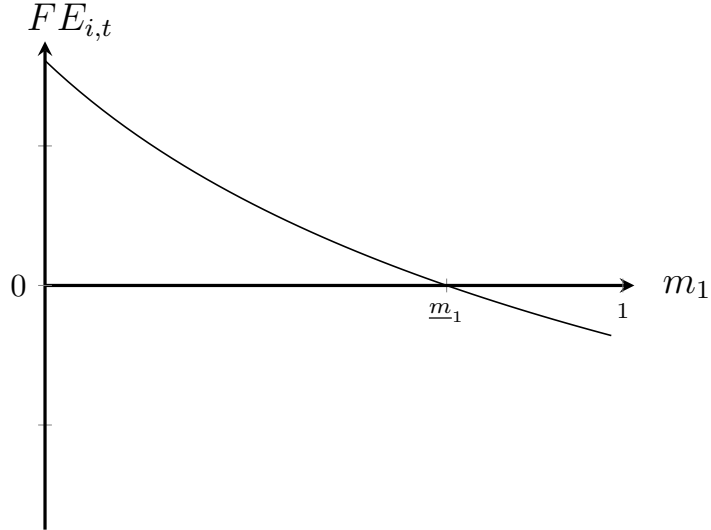


Figure 6.2. Now-cast Error in Period t and Extent of Overreaction.

Note: The figure illustrates how the now-cast error changes with varying degrees of overreaction, given a positive separation error carried over from the previous period $t - 1$.

effect of the cyclical prior is positive in Equation (22).

To illustrate, we consider a scenario where the overconfident forecaster inherits a positive separation error from the previous period (i.e., $z_{i,t-1} > 0$). We start with the extreme case where $m_1 = 0$. In this case, the forecaster's trend belief relies entirely on the newly observed trend signal in the current period t . Consequently, their now-casts are unaffected by trend priors. The inherited separation error affects the now-cast of the current period only through the cyclical prior. As a result, a positive separation error decreases the cyclical prior and correspondingly the now-cast, resulting in a positive now-cast error.

As m_1 increases, indicating a decrease in the extent of overconfidence, forecasters give more weight to trend priors. In this scenario, a positive separation error, which corresponds to a higher trend prior, drives the now-casts to rise and the now-cast error to decline. When $m_1 > \underline{m}_1$, the influence of the trend prior becomes dominant, leading to a negative now-cast error. Therefore, the covariance between the separation error and the now-cast error is negative if and only if $\underline{m}_1 < m_1$.¹³

To summarize, Part (i) of Proposition 4 states that when both the confusion and overconfidence mechanisms are present, the now-cast errors can be positively correlated over time, on condition that the extent of overconfidence in the trend signal is moderate and smaller than a threshold. Table 6.2 summarizes the correlations between the now-cast error in the previous period, the now-cast error in the current period, and the separation error.

¹³When $m_1 = 1$, it reduces to the Bayesian case, and the covariance $\text{cov}(z_{i,t-1}, FE_{i,t})$ is still negative. In this case, since $\text{cov}(z_{i,t-1}, FE_{i,t-1}) = 0$, we have still $\text{cov}(FE_{i,t-1}, FE_{i,t}) = 0$.

Table 6.2. Overconfidence, Confusion and Forecast Error Persistence

Overconfident	$Cov(FE_{i,t-1}, z_{i,t-1})$	$Cov(z_{i,t-1}, FE_{i,t})$	$Cov(FE_{i,t-1}, FE_{i,t})$
Trend signal	Negative	Negative, iif. $\underline{m}_1 < m_1$	Positive, iif. $\underline{m}_1 < m_1 < 1$
Cyclical signal	Positive	Positive, iif. $\underline{m}_2 < m_2$	Positive, iif. $\underline{m}_2 < m_2 < 1$

Furthermore, note that the inequality in Equation (19) characterizes the condition under which the effect of the trend prior dominates the effect of the cyclical prior. Consider the case where the cyclical is very volatile, that is, σ_x^2 is large enough and as a result \underline{m}_1 converges to zero. Forecasters would place very limited reliance on the prior belief regarding the cyclical component and rely heavily on new information about the cycle. Therefore, the effect of the trend prior always dominates, which drives a negative correlation between the separation error and the now-cast error of the current period. As a result, the covariance between the now-cast errors across periods is positive for any $m_1 < 1$.

The analysis of the case where forecasters are overconfident about the cyclical signal is analogous. We relegate the relevant discussion in Appendix C.2.

7 Discussions

In this section, we discuss several alternative modeling approaches and demonstrate the robustness of our framework. Our benchmark model deliberately employs a simplified information structure to highlight the core mechanism at work, but the insights extend to more elaborated specifications.

First, we examine the case where forecasters not only observe the actual state value but also the forecasts made by their peers across various horizons. That is, we assume that at the end of period t , forecaster i observes both the current period's actual state value and the distribution of $F_{i,t}y_{t+h}$ across all forecasters. We will show that this additional information enhances the forecasters' estimates regarding both trend and cyclical components. However, despite this expanded information set, forecasters still cannot perfectly distinguish between the trend and cyclical components.

The key intuition is as follows. In our model, the individual forecast error comprises both the individual-specific forecast error and the common forecast error. The individual-specific forecast error arises from the noise term in the private signals (i.e., $\epsilon_{i,t}$ and $e_{i,t}$), while the common forecast error arises from the state innovations (i.e., γ_t^μ and γ_t^x). The observation of forecasts from others helps to eliminate the individual-specific error and reduce the separation error. Consequently, forecaster i would anchor to the consensus beliefs after observing the entire distribution, as it includes only the

common forecast error. Appendix C.3 provides a complete characterization.

After observing the forecasts of others, the separation error, $z_{i,t}$, becomes common across all forecasters (i.e., $z_{i,t} = z_{j,t}$ for any i, j). We denote this common separation error as z_t . Importantly, we show that z_t is a weighted average of the consensus forecast errors regarding the two components and only includes the state innovations, which is non-zero. This implies that they still cannot perfectly separate the trend and cyclical components, and the key results from our benchmark model continue to hold.

Second, we examine a scenario in which forecasters cannot observe the actual state value or the signals directly related to the trend and cyclical components. Instead, in each period, they receive a private, noisy signal of the state variable y_t . In this context, similar to our model, the covariance between changes in long-run beliefs and cyclical beliefs can be either negative or positive. However, forecast dispersion across forecasters always decreases as the forecast horizon extends.

The key intuition is as follows. In our model, the negative covariance between trend beliefs and cyclical beliefs arises from both state innovations and signal noise. When analyzing the covariance between changes in long-run and cyclical beliefs, both channels play a crucial role, since either a larger trend state innovation or a larger trend signal can lead to a higher trend belief and a lower cyclical belief. Regarding forecast dispersion, since state innovation affects all forecasters equally, it does not influence the dispersion. Only the channel from private signals remains influential, which is captured by ϕ^{COV} in Equation (15). If one forecaster receives a higher trend signal than others, the forecaster will exhibit both a higher trend belief and a lower cyclical belief than the average. This is the key mechanism drives the increasing forecast dispersion.

In contrast, in the alternative setting where forecasters only observe a noisy signal regarding the state variable y_t , the private signal affects trend and cyclical beliefs in the same direction. A large positive signal surprise could indicate both a large trend innovation and a large cyclical innovation. Consequently, if one forecaster receives a higher signal than others, that forecaster will have both a higher trend belief and a higher cyclical belief than the average, thus eliminating the previously mentioned key mechanism. In Appendix C.4, we present a simple example to illustrate the intuition.

Second, we examine an alternative approach to modeling trend-cycle confusion and compare its implications with those of our model. Specifically, we consider a scenario where the source of confusion arises from misinterpreting signals. In this model, forecasters can observe both components at the end of each period. However, they may misinterpret the signals before making forecasts, mistaking a trend signal for a cyclical one or vice versa. We summarize the findings and intuitions below; a detailed illustration is available upon request.

In one such model, forecast dispersion may increase as the forecast horizon extends under certain conditions. The confusion between trends and cycles arises from only a

fraction of forecasters misinterpreting the signals, which leads to a negative covariance between the cross-forecaster mean trend and cyclical beliefs at the aggregate level. For instance, when a positive trend signal is given, a group of forecasters misinterprets it as a cyclical signal. This misinterpretation results in lower mean trend beliefs across all forecasters than would be the case without misinterpretation, and higher mean cyclical beliefs across all forecasters. This mechanism weakens over the forecast horizon, constituting a force that drives up forecast dispersion.

However, in this alternative model, the covariance between an individual's trend beliefs and cyclical beliefs is zero ($\widetilde{COV} = 0$); therefore, the covariance between changes in long-term and cyclical forecasts is always positive ($COV_F^h \geq 0$), which contradicts our empirical findings. This occurs because forecasters can perfectly separate the two components at the end of each period (i.e., $\sigma_z^2 = 0$). Therefore, forecasters would update their beliefs regarding the trend and cyclical components independently, a key difference from our model.

8 Conclusion

This paper introduces a framework where forecasters face rational confusion in distinguishing between trend and cyclical components of state variables. We show that this key feature accounts for a range of forecasting patterns at both individual and aggregate levels. Our quantitative validation examines the 2012 inflation targeting policy, demonstrating that the resulting changes in empirical forecasting behavior align with our model's predictions.

We further show how our framework accommodates behavioral biases, with the interaction between rational confusion and overconfidence accounting for persistent now-cast errors – a notable puzzle in expectation formation literature.

The applications of this framework extend beyond forecasting to any context where individuals have to disentangle two persistent but imperfectly separable processes. Potential applications include investors separating sectoral from firm-specific earnings components, or voters distinguishing between candidate quality and circumstantial factors. We leave the development of those applications to future work.

References

Almeida, H., M. Campello, and M. S. Weisbach (2004). The cash flow sensitivity of cash. *The Journal of Finance* 59(4), 1777–1804.

Andrade, P., R. K. Crump, S. Eusepi, and E. Moench (2016). Fundamental disagreement. *Journal of Monetary Economics* 83, 106–128.

Angeletos, G.-M. and Z. Huo (2021). Myopia and anchoring. *American Economic Review* 111(4), 1166–1200.

Antolin-Diaz, J., T. Drechsel, and I. Petrella (2017). Tracking the slowdown in long-run gdp growth. *Review of Economics and Statistics* 99(2), 343–356.

Blanchard, O. J. and L. H. Summers (1986). Hysteresis and the european unemployment problem. *NBER Macroeconomics Annual* 1, 15–78.

Bordalo, P., N. Gennaioli, Y. Ma, and A. Shleifer (2020). Overreaction in macroeconomic expectations. *American Economic Review* 110(9), 2748–2782.

Bostancı, G. and G. Ordoñez (2024). Business, liquidity, and information cycles.

Broer, T. and A. N. Kohlhas (2024). Forecaster (mis-) behavior. *Review of Economics and Statistics* 106(5), 1334–1351.

Carvalho, C., S. Eusepi, E. Moench, and B. Preston (2023). Anchored inflation expectations. *American Economic Journal: Macroeconomics* 15(1), 1–47.

Chen, H., X. Li, G. Pei, and Q. Xin (2024). Heterogeneous overreaction in expectation formation: Evidence and theory. *Journal of Economic Theory*, 105839.

Chernozhukov, V. and H. Hong (2003). An mcmc approach to classical estimation. *Journal of Econometrics* 115(2), 293–346.

Cogley, T. and T. J. Sargent (2005). Drifts and volatilities: monetary policies and outcomes in the post wwii us. *Review of Economic dynamics* 8(2), 262–302.

Cogley, T. and A. M. Sbordone (2008). Trend inflation, indexation, and inflation persistence in the new keynesian phillips curve. *American Economic Review* 98(5), 2101–2126.

Coibion, O. and Y. Gorodnichenko (2015). Information rigidity and the expectations formation process: A simple framework and new facts. *American Economic Review* 105(8), 2644–2678.

Collard, F., H. Dellas, and F. Smets (2009). Imperfect information and the business cycle. *Journal of Monetary Economics* 56, S38–S56.

Daniel, K., D. Hirshleifer, and A. Subrahmanyam (1998). Investor psychology and security market under-and overreactions. *Journal of Finance* 53(6), 1839–1885.

Delle Monache, D., A. De Polis, and I. Petrella (2024). Modeling and forecasting macroeconomic downside risk. *Journal of Business & Economic Statistics* 42(3), 1010–1025.

Farmer, L. E., E. Nakamura, and J. Steinsson (2024). Learning about the long run. *Journal of Political Economy* 132(10), 3334–3377.

Fisher, J. D., L. Melosi, and S. Rast (2025). Long-run inflation expectations.

Folland, G. B. (2009). *Fourier analysis and its applications*, Volume 4. American Mathematical Soc.

Furlanetto, F., A. Lepetit, Ø. Robstad, J. Rubio-Ramírez, and P. Ulvedal (2025). Estimating hysteresis effects. *American Economic Journal: Macroeconomics* 17(1), 35–70.

Goodfriend, M. (2004). Inflation targeting in the united states? In *The inflation-targeting debate*, pp. 311–352. University of Chicago Press.

Harvey, A. C. (1985). Trends and cycles in macroeconomic time series. *Journal of Business & Economic Statistics*, 216–227.

Huo, Z., M. Pedroni, and G. Pei (2024). Bias and sensitivity under ambiguity. *American Economic Review* 114(12), 4091–4133.

Kohlhas, A. N. and A. Walther (2021). Asymmetric attention. *American Economic Review* 111(9), 2879–2925.

Lahiri, K. and X. Sheng (2008). Evolution of forecast disagreement in a bayesian learning model. *Journal of Econometrics* 144(2), 325–340.

Lorenzoni, G. (2009). A theory of demand shocks. *American Economic Review* 99(5), 2050–2084.

Lucas, R. E. and E. C. Prescott (1978). Equilibrium search and unemployment. In *Uncertainty in economics*, pp. 515–540.

Ma, Y., T. Ropele, D. Sraer, and D. Thesmar (2020). A quantitative analysis of distortions in managerial forecasts.

Muth, J. F. (1960). Optimal properties of exponentially weighted forecasts. *Journal of the American Statistical Association* 55(290), 299–306.

Nelson, C. R. and C. R. Plosser (1982). Trends and random walks in macroeconomic time series: some evidence and implications. *Journal of monetary economics* 10(2), 139–162.

Patton, A. J. and A. Timmermann (2010). Why do forecasters disagree? lessons from the term structure of cross-sectional dispersion. *Journal of Monetary Economics* 57(7), 803–820.

Rozsypal, F. and K. Schlaefmann (2023). Overpersistence bias in individual income expectations and its aggregate implications. *American Economic Journal: Macroeconomics* 15(4), 331–371.

Shapiro, A. and D. J. Wilson (2019). The evolution of the fomc's explicit inflation target. *Evolution* 2019, 12.

Stock, J. H. and M. W. Watson (1998). Median unbiased estimation of coefficient variance in a time-varying parameter model. *Journal of the American Statistical Association* 93(441), 349–358.

Wang, T. and C. Hou (2024). Uncovering subjective models from survey expectations. *Available at SSRN* 3728884.

Xie, S. (2023). An estimated model of household inflation expectations: Information frictions and implications. *Review of Economics and Statistics*, 1–45.

Appendix

A Data and Robustness Tests

A.1 Sample periods and variable definition

The data used in this paper are from the Survey of Professional Forecasters (SPF). Table A.1 provides a list of the periods for which each forecast variable is available.

Table A.1. Summary of sample periods

Summary of sample periods	
Forecast Variable	Sample periods
Panel A. Short-term Forecasts.	
Nominal GDP	1968Q4 - 2019Q4
Real GDP	1968Q4 - 2019Q4
GDP price index inflation	1968Q4 - 2019Q4
Real consumption	1981Q3 - 2019Q4
Industrial production	1968Q4 - 2019Q4
Real nonresidential investment	1981Q3 - 2019Q4
Real residential investment	1981Q3 - 2019Q4
Real federal government consumption	1981Q3 - 2019Q4
Real state and local government consumption	1981Q3 - 2019Q4
Housing start	1968Q4 - 2019Q4
Unemployment	1968Q4 - 2019Q4
Inflation (CPI)	1981Q3 - 2019Q4
Three-month Treasury rate	1981Q3 - 2019Q4
Ten-year Treasury rate	1992Q1 - 2019Q4
Panel B. Long-term Forecasts.	
Three-year ahead Real GDP	2009Q2-2019Q4
Three-year ahead unemployment	2009Q2-2019Q4
Ten-year ahead inflation (CPI)	1991Q3-2019Q4
Ten-year ahead Real GDP	1992Q1-2019Q1; first quarter only
Natural rate of unemployment	1996Q3-2019Q3; third quarter only

Following Bordalo et al. (2020), we convert macroeconomic variables to annual growth rates. For variables that are already presented as rates, we use the original data directly.

Variables changed to the annual growth rate include nominal GDP (NGDP), real GDP (RGDP), GDP price index inflation (PGDP), real consumption (RCONSUM), Industrial production (INDPROD), real nonresidential investment (RNRESIN), real residential investment (RRESINV), real federal government consumption (RGF), real state and local government consumption (RGSL). Forecast of h period ahead: $F_{i,t}y_{t+h} = \left(\frac{F_{i,t}\tilde{y}_{t+h}}{\tilde{y}_{t+h-4}} - 1\right) \times 100$, where $F_{i,t}\tilde{y}_{t+h}$ is the original survey forecast from the forecaster i provided in period t regarding the state variable \tilde{y} in h period ahead. \tilde{y}_{t+h-4} is the actual state value of period $t + h - 4$ already released. The procedures are a replication of Bordalo et al. (2020).

Variables that are taken directly from the survey data include unemployment rate

(UNEMP), housing start (HOUSING), CPI, Three-month Treasury rate (Tbills), Ten-year Treasury rate (Tbonds).

A.2 Three years ahead forecast and forecasts of longer horizon

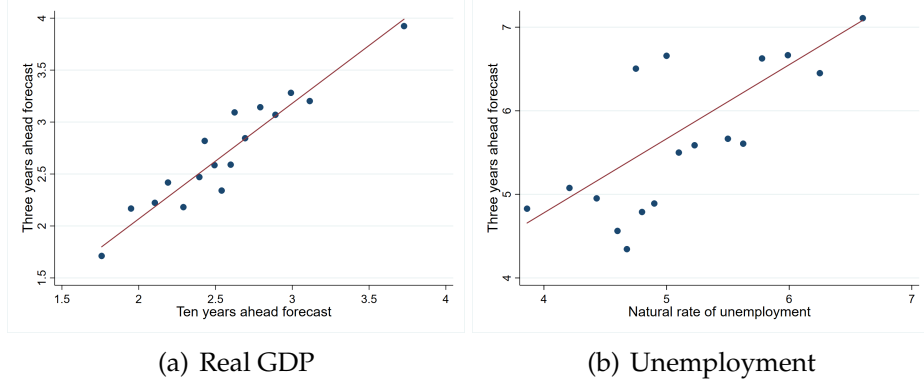


Figure A.1. Three-year-ahead forecasts and forecasts for longer horizons. Note: The sample period is from 2009 to 2019, based on data availability. Forecasts of the natural unemployment rate are only available in the third quarter survey, while forecasts of ten-year-ahead real GDP are only available in the first quarter survey. Figure 1(a) illustrates the real GDP forecasts for three years ahead and ten years ahead. Figure 1(b) shows unemployment forecasts for three years ahead and the natural rate of unemployment. The correlation between the three-year horizon forecasts and longer-horizon forecasts, as depicted in the upper two figures, is 0.903 for real GDP growth and 0.886 for unemployment.

A.3 Estimation Results: Covariance between changes in long-term forecasts and cyclical forecasts

Table A.2. Covariance between changes in long term forecasts and cyclical forecasts

Covariance between changes in long term forecasts and cyclical forecasts			
	COV_F^h	95% bootstrap CI	Obs
Panel A. Unemployment rate			
$h = 0$	-0.203	(-0.244, -0.161)	794
$h = 1$	-0.192	(-0.232, -0.152)	815
$h = 2$	-0.177	(-0.214, -0.139)	819
$h = 3$	-0.164	(-0.199, -0.129)	817
$h = 4$	-0.151	(-0.183, -0.118)	818
Panel B. Real GDP growth			
$h = 0$	-0.219	(-0.273, -0.164)	783
$h = 1$	-0.214	(-0.271, -0.156)	781
$h = 2$	-0.204	(-0.260, -0.147)	785
$h = 3$	-0.204	(-0.258, -0.149)	785
$h = 4$	-0.202	(-0.256, -0.148)	785

Note: This table shows the covariance between the changes in long-term forecasts and cyclical forecasts. The sample period is from 2009Q2 to 2019Q4. Panel A shows the results of the unemployment rate, while Panel B shows the results of the Real GDP growth.

A.4 Robustness: ECB-SPF

This subsection presents estimation results using the European Central Bank's Survey of Professional Forecasters (ECB-SPF). The ECB-SPF is a quarterly survey collecting

data on expected inflation, real GDP growth, and unemployment rates in the euro area. Each quarter, approximately 50 professional forecasters participate, providing forecasts for the current and following year. Forecasts for two years ahead were available only in Q3 and Q4 surveys from 2001 to 2012, but have been included in all survey waves since 2013. Since 2001, the survey has included a question on long-term economic conditions. This question solicits forecasts for four years ahead in Q1 and Q2 surveys, and five years ahead in Q3 and Q4 surveys. We use these four- and five-year-ahead forecasts as our long-run forecasts.

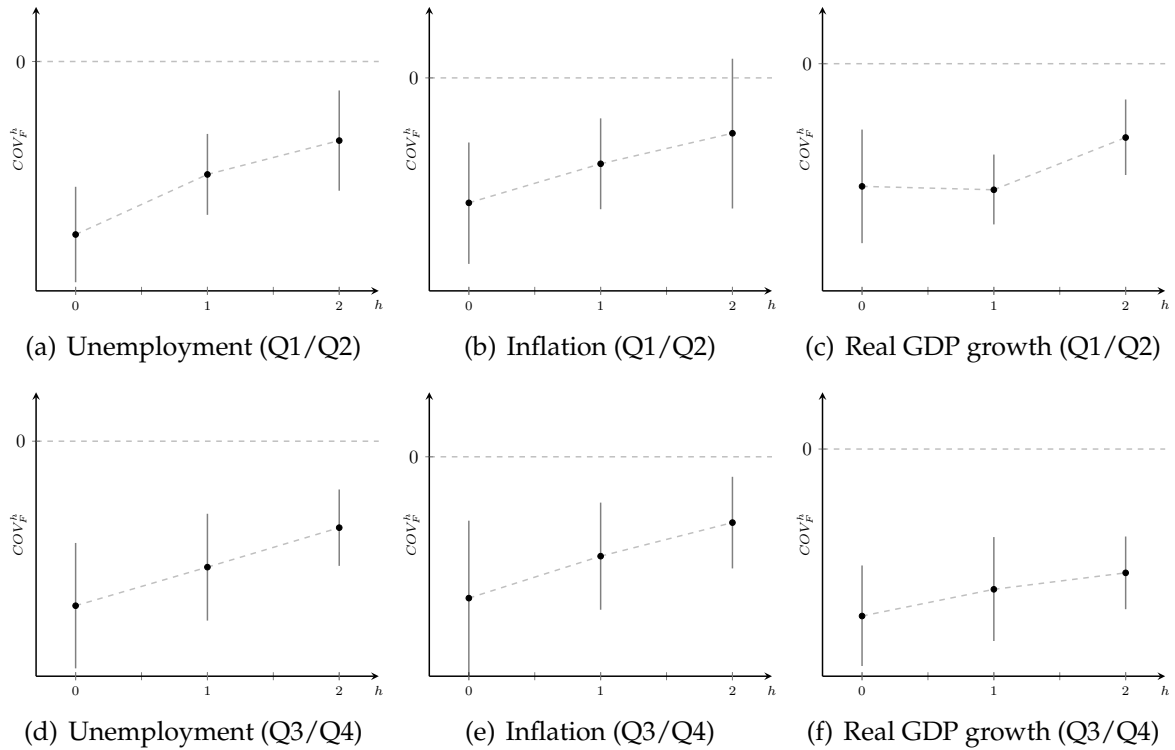


Figure A.2. Covariance between the changes in long-run forecasts and cyclical forecasts across forecast horizons h . Note: This figure illustrates the covariance COV_F^h for the unemployment rate, inflation and the real GDP growth across various forecast horizons h using the ECB-SPF data. The upper three figures show the estimation result using the Q1 and Q2 data. The lower three figures show the estimation result using the Q3 and Q4 data. In all cases, the covariance is negative and statistically significant, increasing as the forecast horizon extends. The black dots represent the estimates, and the gray solid lines denote the 95% confidence intervals. The sample period is from 2001Q1 to 2019Q4.

Figure A.2 presents the estimation results of Equation (1) using ECB-SPF data. Horizons $h = 0, 1, 2$ correspond to forecasts for the current year, one year ahead, and two years ahead, respectively. Because Q1/Q2 surveys request forecasts four years ahead, while Q3/Q4 surveys request forecasts five years ahead, we split the data into two subsamples. The upper panels of Figure A.2 use the Q1/Q2 subsample (cyclical belief = h -horizon forecast minus four-year-ahead forecast). The lower panels use the Q3/Q4 subsample (cyclical belief = h -horizon forecast minus five-year-ahead forecast).

For all variables, the estimated coefficients COV_F^0 are negative, statistically significant, and increasing in h , consistent with the results in the main text.

Table A.3 presents the estimation results from Equation (2) using ECB-SPF data. These results are consistent with those in the main text. For unemployment and real GDP growth, the estimated coefficients are statistically positive. For inflation, the coefficient is statistically positive but small when using forecast variance as the dispersion measure, and non-significant when using the interquartile range (75th minus 25th percentile).

Table A.3. Forecast dispersion over forecast horizon

Forecast Variable	Dependent Variable: Forecast Dispersion				
	Variance of forecasts		50 percentile difference		Obs
	β_1	SE	β_1	SE	
(1)	(2)	(3)	(4)		
Unemployment rate	0.122***	0.006	0.182***	0.007	280
Real GDP growth	0.006***	0.002	0.022***	0.005	280
Inflation rate	0.003**	0.001	0.002	0.004	280

Note: This table shows results from estimating Equation (2) using the ECB-SPF data. The sample period is from 2001Q1 to 2019Q4. In column (1), the dependent variable is the variance of forecasts across forecasters. In column (3), we use the difference between the 25% percentile and 50% percentile. Standard errors are clustered at the year-quarter level.

A.5 Robustness: Forecast dispersion over forecast horizon with time fixed effect

Table A.4. Forecast dispersion over forecast horizon with time FE

Forecast Variable	Dependent Variable: Forecast Dispersion					
	Variance of forecasts		50 percentile difference		Time FE	Obs
	β_1	SE	β_1	SE		
(1)	(2)	(3)	(4)			
Nominal GDP	0.337***	0.014	0.204***	0.005	Yes	1,025
Real GDP	0.242***	0.013	0.162***	0.004	Yes	1,025
GDP price index inflation	0.118***	0.005	0.119***	0.003	Yes	1,025
Real consumption	0.125***	0.008	0.127***	0.004	Yes	770
Industrial production	0.860***	0.034	0.320***	0.009	Yes	1,025
Real nonresidential investment	1.647***	0.068	0.497***	0.012	Yes	770
Real residential investment	6.021***	0.299	0.932***	0.026	Yes	770
Real federal government consumption	1.284***	0.065	0.393***	0.013	Yes	770
Real state and local government consumption	0.317***	0.016	0.210***	0.006	Yes	770
Housing start	0.004***	0.000	0.020***	0.001	Yes	1,024
Unemployment	0.034***	0.001	0.082***	0.002	Yes	1,014
Inflation rate (CPI)	-0.066***	0.013	-0.073***	0.008	Yes	770
Three-month Treasury rate	0.053***	0.002	0.106***	(0.003)	Yes	770
Ten-year Treasury rate	0.045***	0.001	0.094***	0.002	Yes	560

Note: This table shows the coefficients from estimating Equation (2) with year-quarter fixed effect. The sample period is from 1968Q4 to 2019Q4. In column (1), the dependent variable is the variance of forecasts. In column (3), the dependent variable is the difference between the 25% percentile and 50% percentile. Standard errors are clustered at the year-quarter level.

A.6 Estimation procedures: Inflation

To estimate the set of parameters $\Theta = \{\rho, \sigma_\mu^2, \sigma_x^2, \sigma_e^2, \sigma_\epsilon^2\}$ before and after 2012, we begin by dividing the entire dataset into two subsets: one before 2012 and one after 2012. For each subset, we compute the average forecast variance for different forecast horizons ($h = 0, 1, 2, 3, 4$). These sets of forecast variances serve as the targets for estimation denoted as \hat{m} .

Since we want to capture the forecast variance across all the horizons, we give equal weights to all the targeted moments. Table A.5 provides the summary statistic of the estimation moments.

Table A.5. Estimation Moments

Estimation Moments				
	Pre-2012		Post-2012	
	Target	SE	Target	SE
h=0	0.833	1.276	0.737	0.693
h=1	0.562	0.568	0.350	0.182
h=2	0.464	0.370	0.303	0.123
h=3	0.429	0.324	0.284	0.103
h=4	0.430	0.282	0.301	0.071

The distance is defined in Equation (17) as the weighted squared difference between the target moments \hat{m} and the model prediction $m(\Theta)$, which represents the moments implied by the model for the given parameter set (Θ). Using MCMC with the Metropolis-Hastings algorithm, we choose the set of model parameters that minimize the distance $\Lambda(\Theta)$. The estimation of the parameter set before and after 2012 follows the exact same procedures, with different estimation targets derived from the respective subsets of the data.

B Proofs

Characterization of special case when the trend is observable in section 4.1.

Consider a special case where both the state and trend components are observable at the end of each period. Without loss of generality, we assume the cyclical component follows an AR(N) process:

$$x_t = \sum_{h=0}^N \rho^h L^h x_t + \gamma_t^x,$$

where L is the lag operator.

The private signal of forecaster i is given by:

$$s_{i,t}^{\mu} = \mu_t + \epsilon_{i,t} \quad \text{and} \quad s_{i,t}^x = x_t + e_{i,t}.$$

Given the trend component is observable at the end of each period, one's prior belief before observing the signals is:

$$\theta_{2,t-1}^i = \begin{pmatrix} \mu_{t-1} \\ \sum_{h=0}^N \rho^h L^h x_t \end{pmatrix}.$$

The posterior beliefs regarding the two components upon observing the signals is given by:

$$\theta_{1,t}^i = \theta_{2,t-1}^i + \kappa \times (s_{i,t} - \theta_{2,t-1}^i),$$

where the Kalman gain matrix and the variance-covariance matrix is same as the ones in the main text:

$$\kappa = \begin{pmatrix} \frac{\sigma_{\mu}^2}{\sigma_{\mu}^2 + \sigma_{\epsilon}^2} & 0 \\ 0 & \frac{\sigma_x^2}{\sigma_x^2 + \sigma_{\epsilon}^2} \end{pmatrix}, \quad \text{and} \quad \begin{pmatrix} \text{Var}_s^T & \widetilde{\text{COV}}_s \\ \widetilde{\text{COV}}_s & \text{Var}_s^C \end{pmatrix} = \begin{pmatrix} \frac{\sigma_{\epsilon}^2 \sigma_{\mu}^2}{\sigma_{\epsilon}^2 + \sigma_{\mu}^2} & 0 \\ 0 & \frac{\sigma_{\epsilon}^2 \sigma_x^2}{\sigma_x^2 + \sigma_{\epsilon}^2} \end{pmatrix}.$$

The forecast variance across forecasters is given by:

$$\begin{aligned} E[(F_{i,t} y_{t+h} - \bar{E}[F_{i,t} y_{t+h}])^2] &= \rho^{2h} \underbrace{\frac{\sigma_x^2}{\sigma_x^2 + \sigma_{\epsilon}^2} \text{Var}_s^C}_{\phi_s^C} + \underbrace{\frac{\sigma_{\mu}^2}{\sigma_{\mu}^2 + \sigma_{\epsilon}^2} \text{Var}_s^T}_{\phi_s^T} \\ &= \rho^{2h} \left(\frac{\sigma_x^2}{\sigma_x^2 + \sigma_{\epsilon}^2} \right)^2 \sigma_{\epsilon}^2 + \left(\frac{\sigma_{\mu}^2}{\sigma_{\mu}^2 + \sigma_{\epsilon}^2} \right)^2 \sigma_{\epsilon}^2. \end{aligned}$$

It is evidence that the forecast variance across forecasters is decreasing, as the forecast horizon extends.

In addition, changes in trend forecasts and changes cyclical forecasts can be written as follows:

$$F_{i,t} y_{t+3Y} - F_{i,t-1} y_{t-1+3Y} = (\mu_{1,t}^i - E_{i,t-1}[\mu_{t-1}]) + \rho^{3Y} (E_{i,t}[\sum_{h=0}^N \rho^h L^h x_{t+3Y}] - E_{i,t-1}[\sum_{h=0}^N \rho^h L^h x_{t+3Y-1}]),$$

and

$$Cyc_{i,t} - Cyc_{i,t-1} = (1 - \rho^{3Y}) (E_{i,t}[\sum_{h=0}^N \rho^h L^h x_{t+3Y}] - E_{i,t-1}[\sum_{h=0}^N \rho^h L^h x_{t+3Y-1}]).$$

Following the same logic as the main text, the covariance between changes in the beliefs about the trend component and changes in beliefs about the cyclical component

at any horizon should be non-negative. That is,

$$\begin{aligned} & COV_F^h(F_{i,t}y_{t+3Y} - F_{i,t-1}y_{t-1+3Y}, Cyc_{i,t} - Cyc_{i,t-1}) \\ &= \rho^{3Y}(1 - \rho^{3Y})Var(E_{i,t}[\sum_{h=0}^N \rho^h L^h x_{t+3Y}] - E_{i,t-1}[\sum_{h=0}^N \rho^h L^h x_{t+3Y-1}]) \geq 0. \end{aligned}$$

In this special case, where trends and cycles are observable at the end of each period, the model fails to replicate either of the two empirical patterns documented, even when we allow the data generation process for the cyclical component to follow an AR(N) process.

Proof of Lemma 1. To begin, we assume that the error term in the last period ($z_{i,t-1}$) is normally distributed with the variance $\sigma_{z,t-1}^2$. With the prior belief and the signal structures given by Equation (6) and (7), the posterior belief of forecaster i after receiving signals is given by:

$$\begin{aligned} p(\theta|s_{i,t}) &\propto p(\theta_{2,t-1}^i)p(s_{i,t}|\theta_{2,t-1}^i) \\ &\propto \exp\left\{-\frac{1}{2}[\theta^T(\Sigma_s^{-1} + \Sigma_{\theta_{2,t-1}^i}^{-1})\theta - 2(\Sigma_s^{-1} + \Sigma_{\theta_{2,t-1}^i}^{-1})^{-1}(\Sigma_s^{-1} + \Sigma_{\theta_{2,t-1}^i}^{-1})(s_{i,t}^T \Sigma_s^{-1} + \theta_{2,t-1}^{i,T} \Sigma_{\theta_{2,t-1}^i}^{-1})\theta]\right\} \\ &\propto \exp[-\frac{1}{2}(\theta - \theta_{1,t}^i)^T(\Sigma_s^{-1} + \Sigma_{\theta_{2,t-1}^i}^{-1})(\theta - \theta_{1,t}^i)], \end{aligned}$$

where

$$\theta_{1,t}^i = (\Sigma_s^{-1} + \Sigma_{\theta_{2,t-1}^i}^{-1})^{-1}(s_{i,t}^T \Sigma_s^{-1} + \theta_{2,t-1}^{i,T} \Sigma_{\theta_{2,t-1}^i}^{-1})^T.$$

Therefore, $\mu_{1,t}^i$ and $x_{1,t}^i$ are joint normally distributed. To be specific, $\theta_{1,t}^i = (\mu_{1,t}^i, x_{1,t}^i)'$ is given by:

$$\mu_{1,t}^i = \underbrace{\frac{\sigma_e^2(\rho^2\sigma_{z,t-1}^2 + \sigma_x^2 + \sigma_e^2)}{\Omega_t} \mu_{2,t-1}^i}_{\text{prior weight}} + \underbrace{\frac{V_t + \sigma_e^2(\sigma_{z,t-1}^2 + \sigma_\mu^2)}{\Omega_t} s_{i,t}^\mu}_{\text{signal weight}} - \underbrace{\frac{\rho\sigma_e^2\sigma_{z,t-1}^2}{\Omega_t} (s_{i,t}^x - \rho x_{2,t-1}^i)}_{\text{surprise from cycle}}, \quad (B1)$$

$$x_{1,t}^i = \underbrace{\frac{\sigma_e^2(\sigma_{z,t-1}^2 + \sigma_\mu^2 + \sigma_e^2)}{\Omega_t} \rho x_{2,t-1}^i}_{\text{prior weight}} + \underbrace{\frac{V_t + \sigma_e^2(\sigma_x^2 + \rho^2\sigma_{z,t-1}^2)}{\Omega_t} s_{i,t}^x}_{\text{signal weight}} - \underbrace{\frac{\rho\sigma_e^2\sigma_{z,t-1}^2}{\Omega_t} (s_{i,t}^\mu - \mu_{2,t-1}^i)}_{\text{surprise from trend}}. \quad (B2)$$

where Ω_t and V_t are constants:

$$\Omega_t = (\sigma_{z,t-1}^2 + \sigma_\mu^2 + \sigma_e^2)(\sigma_x^2 + \sigma_e^2 + \rho^2\sigma_{z,t-1}^2) - \rho^2\sigma_{z,t-1}^4, \quad V_t = (\sigma_{z,t-1}^2 + \sigma_\mu^2)(\sigma_x^2 + \rho^2\sigma_{z,t-1}^2) - \rho^2\sigma_{z,t-1}^4.$$

And the variance-covariance matrix of $\mu_{1,t}^i$ and $x_{1,t}^i$ is:

$$(\Sigma_s^{-1} + \Sigma_{\theta_{2,t-1}^i}^{-1})^{-1} = \begin{pmatrix} \text{Var}_t^T & \widetilde{\text{COV}}_t \\ \widetilde{\text{COV}}_t & \text{Var}_t^C \end{pmatrix} = \begin{pmatrix} \frac{\sigma_e^2[\Omega_t - \sigma_e^2(\sigma_x^2 + \sigma_e^2 + \rho^2 \sigma_{z,t-1}^2)]}{\Omega_t} & -\frac{\rho \sigma_e^2 \sigma_e^2 \sigma_{z,t-1}^2}{\Omega_t} \\ -\frac{\rho \sigma_e^2 \sigma_e^2 \sigma_{z,t-1}^2}{\Omega_t} & \frac{\sigma_e^2[\Omega_t - \sigma_e^2(\sigma_e^2 + \sigma_\mu^2 + \sigma_{z,t-1}^2)]}{\Omega_t} \end{pmatrix}, \quad (\text{B3})$$

The observation of y_t provides new information and forecasters would update their beliefs accordingly:

$$\begin{aligned} f^i(\mu_t | y_t) &\propto \exp \left\{ -\frac{1}{2(1-r_t^2)} \left[\frac{(\mu_t - \mu_{1,t}^i)^2}{\text{Var}_t^T} - \frac{2r_t(\mu_t - \mu_{1,t}^i)(y_t - \mu_t - x_{1,t}^i)}{\sqrt{\text{Var}_t^T \text{Var}_t^C}} + \frac{(y_t - \mu_t - x_{1,t}^i)^2}{\text{Var}_t^C} \right] \right\} \\ &\propto \exp \left\{ -\frac{1}{2(1-r_t^2)} \left[\frac{(\text{Var}_t^T + 2r_t \sqrt{\text{Var}_t^T \text{Var}_t^C} + \text{Var}_t^C) \mu_t^2}{\text{Var}_t^T \text{Var}_t^C} \right. \right. \\ &\quad \left. \left. - 2\mu_t \frac{\text{Var}_t^C \mu_{1,t}^i + r_t \sqrt{\text{Var}_t^T \text{Var}_t^C} (\mu_{1,t}^i + y_t - x_{1,t}^i) + \text{Var}_t^T (y_t - x_{1,t}^i)}{\text{Var}_t^T \text{Var}_t^C} \right] \right\}, \end{aligned} \quad (\text{B4})$$

and

$$\begin{aligned} f^i(x_t | y_t) &\propto \exp \left\{ -\frac{1}{2(1-r_t^2)} \left[\frac{(y_t - x_t - \mu_{1,t}^i)^2}{\text{Var}_t^T} - \frac{2r_t(y_t - x_t - \mu_{1,t}^i)(x_t - x_{1,t}^i)}{\sqrt{\text{Var}_t^T \text{Var}_t^C}} + \frac{(x_t - x_{1,t}^i)^2}{\text{Var}_t^C} \right] \right\} \\ &\propto \exp \left\{ -\frac{1}{2(1-r_t^2)} \left[\frac{\text{Var}_t^T + 2r_t \sqrt{\text{Var}_t^T \text{Var}_t^C} + \text{Var}_t^T x_t^2}{\text{Var}_t^T \text{Var}_t^C} \right. \right. \\ &\quad \left. \left. - 2x_t \frac{\text{Var}_t^C (y_t - \mu_{1,t}^i) + r_t \sqrt{\text{Var}_t^T \text{Var}_t^C} (y_t - \mu_{1,t}^i + x_{1,t}^i) + \text{Var}_t^T x_{1,t}^i}{\text{Var}_t^T \text{Var}_t^C} \right] \right\}, \end{aligned} \quad (\text{B5})$$

where r_t is given by:

$$r_t = \frac{\widetilde{\text{COV}}_t}{\sqrt{\text{Var}_t^T \text{Var}_t^C}}. \quad (\text{B6})$$

According to Equations (B4) and (B5), the posterior beliefs $f^i(\mu_t | y_t)$ and $f^i(x_t | y_t)$ are normal distributions. Therefore, $\mu_{2,t}^i$ and $x_{2,t}^i$ are normally distributed. As a result, $z_{i,t}$ will also be normally distributed. That shows first part of the lemma.

Furthermore, the means of the posterior beliefs are given by:

$$\begin{aligned}\mu_{2,t}^i &= \frac{\text{Var}_t^C \mu_{1,t}^i + \text{Var}_t^T (y_t - x_{1,t}^i) + r_t \sqrt{\text{Var}_t^T \text{Var}_t^C} (\mu_{1,t}^i + y_t - x_{1,t}^i)}{\text{Var}_t^T + 2r_t \sqrt{\text{Var}_t^T \text{Var}_t^C} + \text{Var}_t^C} \\ &= \frac{(\text{Var}_t^C + \widetilde{\text{COV}}_t) \mu_{1,t}^i + (\text{Var}_t^T + \widetilde{\text{COV}}_t) (y_t - x_{1,t}^i)}{\text{Var}_t^T + \text{Var}_t^C + 2\widetilde{\text{COV}}_t}.\end{aligned}\quad (\text{B7})$$

and

$$\begin{aligned}x_{2,t}^i &= \frac{\text{Var}_t^C (y_t - \mu_{1,t}^i) + r_t \sqrt{\text{Var}_t^T \text{Var}_t^C} (y_t - \mu_{1,t}^i + x_{1,t}^i) + \text{Var}_t^T x_{1,t}^i}{\text{Var}_t^T + 2r_t \sqrt{\text{Var}_t^T \text{Var}_t^C} + \text{Var}_t^C} \\ &= \frac{(\text{Var}_t^C + \widetilde{\text{COV}}_t) (y_t - \mu_{1,t}^i) + (\text{Var}_t^T + \widetilde{\text{COV}}_t) x_{1,t}^i}{\text{Var}_t^T + \text{Var}_t^C + 2\widetilde{\text{COV}}_t}.\end{aligned}$$

We show that

$$\begin{aligned}\mu_{2,t}^i + x_{2,t}^i &= \frac{(\text{Var}_t^C + \widetilde{\text{COV}}_t) \mu_{1,t}^i + (\text{Var}_t^T + \widetilde{\text{COV}}_t) (y_t - x_{1,t}^i)}{\text{Var}_t^T + \text{Var}_t^C + 2\widetilde{\text{COV}}_t} \\ &\quad + \frac{(\text{Var}_t^C + \widetilde{\text{COV}}_t) (y_t - \mu_{1,t}^i) + (\text{Var}_t^T + \widetilde{\text{COV}}_t) x_{1,t}^i}{\text{Var}_t^T + \text{Var}_t^C + 2\widetilde{\text{COV}}_t} \\ &= y_t.\end{aligned}$$

The second part of the lemma is shown.

Proof of Lemma 2. We first establish the existence of the steady state and then show that the steady state is unique. According to Equations (B4) and (B5), after observing y_t , the variance of the separation error is given by:

$$\sigma_{z_t}^2 = \frac{(1 - r_t^2) \text{Var}_t^T \text{Var}_t^C}{\text{Var}_t^T + 2r_t \sqrt{\text{Var}_t^T \text{Var}_t^C} + \text{Var}_t^C}. \quad (\text{B8})$$

Recall the definitions of Var_t^T , Var_t^C and r_t in Equations (B3) and (B6), we notice that the right-hand-side of Equation (B8) is a function of $\sigma_{z,t-1}^2$. Therefore, the steady state value σ_z^2 is a fixed point of the condition characterized by Equation (B8). Solving for the fixed point of Equation (B8) gives:

$$\sigma_z^2 = \frac{-\sigma_\mu^2 [\Lambda + 2\rho(1 - \rho)\sigma_e^2\sigma_\epsilon^2] + \sqrt{\sigma_\mu^2 \Lambda [\sigma_\mu^2 (\Lambda + 4\rho\sigma_e^2\sigma_\epsilon^2) + 4\sigma_e^2\sigma_\epsilon^2\sigma_x^2]}}{2[\Lambda + \rho^2\sigma_\mu^2(\sigma_e^2 + \sigma_\epsilon^2)]}, \quad (\text{B9})$$

where $\Lambda = (1 - \rho)^2 \sigma_e^2 \sigma_\epsilon^2 + \sigma_x^2 (\sigma_e^2 + \sigma_\epsilon^2)$.

In the next step, we demonstrate that regardless of the initial variance of the separation error, denoted as $\sigma_{z_0}^2$, it always converges to a unique steady state value σ_z^2 . We first simplify Equation (B8) to:

$$\sigma_{z,t}^2 = \frac{g_1(\sigma_{z,t-1}^2)}{g_2(\sigma_{z,t-1}^2)}, \quad (\text{B10})$$

where

$$g_1(\sigma_{z,t-1}^2) = w_1 \sigma_{z,t-1}^2 + \eta_1 \quad \text{and} \quad g_2(\sigma_{z,t-1}^2) = w_2 \sigma_{z,t-1}^2 + \eta_2,$$

$$w_1 = \sigma_e^2 \sigma_\epsilon^2 (\rho^2 \sigma_\mu^2 + \sigma_x^2); \quad \eta_1 = \sigma_e^2 \sigma_\epsilon^2 \sigma_\mu^2 \sigma_x^2;$$

$$w_2 = \rho^2 (\sigma_e^2 \sigma_\epsilon^2 + \sigma_e^2 \sigma_\mu^2 + \sigma_\mu^2 \sigma_\epsilon^2) + \sigma_e^2 \sigma_\epsilon^2 + \sigma_e^2 \sigma_x^2 + \sigma_\epsilon^2 \sigma_x^2 - 2\rho \sigma_e^2 \sigma_\epsilon^2; \quad \eta_2 = \sigma_e^2 \sigma_\epsilon^2 (\sigma_\mu^2 + \sigma_x^2) + \sigma_\mu^2 \sigma_x^2 (\sigma_e^2 + \sigma_\epsilon^2).$$

Define the difference between $\sigma_{z,t}^2$ and $\sigma_{z,t-1}^2$ as:

$$D(\sigma_{z,t-1}^2) = \sigma_{z,t}^2 - \sigma_{z,t-1}^2 = \frac{g_1(\sigma_{z,t-1}^2)}{g_2(\sigma_{z,t-1}^2)} - \sigma_{z,t-1}^2.$$

To show the steady state is unique, it is sufficient to show that $D(\sigma_{z,t-1}^2)$ is monotonically decreasing. We first show that evaluated at $\sigma_{z,t-1}^2 = 0$, the derivative is negative.

$$\frac{\partial D(\sigma_{z,t-1}^2)}{\partial \sigma_{z,t-1}^2} \Big|_{\sigma_{z,t-1}^2=0} = \left[\frac{\sigma_e^2 \sigma_\epsilon^2 (\rho \sigma_\mu^2 + \sigma_x^2)}{\sigma_e^2 \sigma_\epsilon^2 (\rho \sigma_\mu^2 + \sigma_x^2) + \sigma_\mu^2 \sigma_x^2 (\sigma_e^2 + \sigma_\epsilon^2)} \right]^2 - 1 < 0.$$

Then we show that the first-order derivative of $D(\sigma_{z,t-1}^2)$ is negative. The derivative is given by:

$$\frac{\partial D(\sigma_{z,t-1}^2)}{\partial \sigma_{z,t-1}^2} = \frac{w_1 \eta_2 - w_2 \eta_1}{(w_2 \sigma_{z,t}^2 + \eta_2)^2} - 1 = \left[\frac{\sigma_e^2 \sigma_\epsilon^2 (\rho \sigma_\mu^2 + \sigma_x^2)}{(w_2 \sigma_{z,t}^2 + \eta_2)} \right]^2 - 1. \quad (\text{B11})$$

It is always decreasing, because we show that the second-order derivative is negative:

$$\frac{\partial^2 D(\sigma_{z,t-1}^2)}{\partial (\sigma_{z,t-1}^2)^2} = -2w_2 \frac{[\sigma_e^2 \sigma_\epsilon^2 (\rho \sigma_\mu^2 + \sigma_x^2)]^2}{(w_2 \sigma_{z,t}^2 + \eta_2)^3} < 0.$$

Since $D(\sigma_{z,t}^2)$ is monotonously decreasing and concave and the steady state exists, it is unique. Figure 1(a) illustrates the relationship between $\sigma_{z,t-1}^2$ and $\sigma_{z,t}^2$, while Figure 1(b) further illustrates how the difference between the two variances (i.e., $\sigma_{z,t}^2 - \sigma_{z,t-1}^2$) responds to $\sigma_{z,t-1}^2$, highlighting the convergence property.

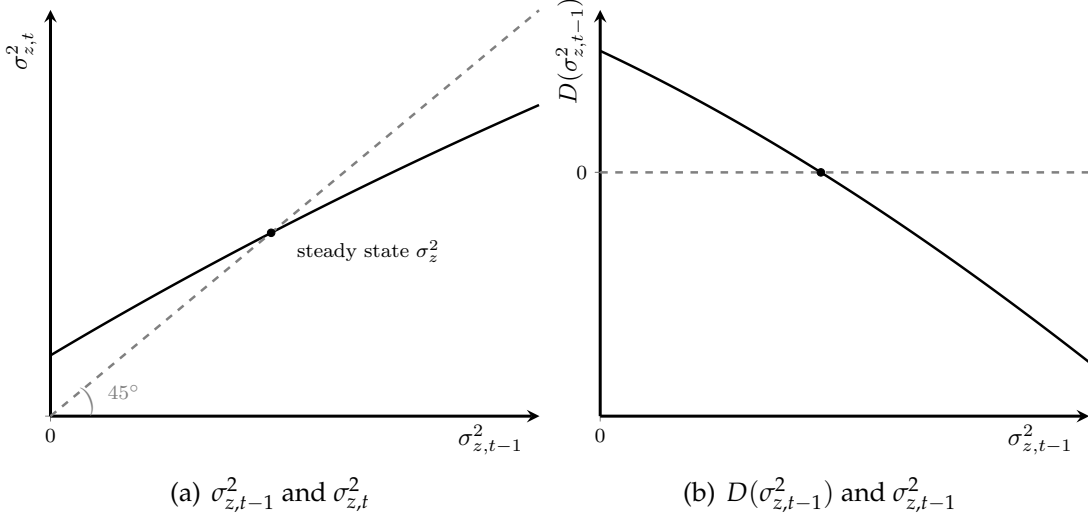


Figure B.1. The relationship between $\sigma_{z,t-1}^2$ and $\sigma_{z,t}^2$.

Proof of Lemma 3. Given the quadratic utility function, the forecaster's optimal forecasts are given by the following:

$$\begin{aligned}
 F_{i,t}y_{t+h} &= E_{i,t}[y_{t+h}] \\
 &= E_{i,t}[\mu_t + \rho^h x_t] \\
 &= \mu_{1,t}^i + \rho^h x_{1,t}^i.
 \end{aligned}$$

The first equality is derived from the first order condition of the standard quadratic utility function. With a quadratic utility function, forecasters would minimize the expected squared error, and the first-order condition is given by:

$$E_{i,t}[F_{i,t}y_{t+h} - y_{t+h}] = 0.$$

The second equality follows given the data generation process is known to forecasters. The third equality states that the expected value of the sum of μ_t and $\rho^h x_t$ is the sum of the expected values of the two components, a well known property using Fourier transform (Folland 2009).

Proof of Lemma 4. From Equation (B7) in the proof of Lemma 2, we obtain:

$$\begin{aligned}
 z_{i,t-1} &= \mu_{2,t-1}^i - \mu_{t-1} \\
 &= \frac{(\text{Var}^T + \widetilde{\text{COV}})(x_{t-1} - x_{1,t-1}^i) - (\text{Var}^C + \widetilde{\text{COV}})(\mu_{t-1} - \mu_{1,t-1}^i)}{\text{Var}^T + \widetilde{\text{COV}} + \text{Var}^C + \widetilde{\text{COV}}},
 \end{aligned}$$

which is the first part of Lemma 4.

For the second part of Lemma 4, we show the steady state value of σ_z^2 increases in σ_μ^2 . Our idea is to show that the solid line in Figure 1(a) shifts upwards when σ_μ^2 is larger. Towards this end, we prove the following claim.

Claim 1. For any given $\sigma_{z,t-1}^2$, the induced $\sigma_{z,t}^2$ is increasing in σ_μ^2 .

Using Equation (B10), we obtain the derivative:

$$\frac{\partial \sigma_{z,t}^2}{\partial \sigma_\mu^2} = \frac{\partial [g_1(\sigma_{z,t-1}^2)/g_2(\sigma_{z,t-1}^2)]}{\partial \sigma_\mu^2} = \frac{\sigma_e^4 \sigma_\epsilon^4 [\sigma_x^2 - \rho(1-\rho)\sigma_{z,t-1}^2]^2}{g_2(\sigma_{z,t-1}^2)^2} > 0. \quad (\text{B12})$$

The claim is shown. Consequently, given the properties of $D(\sigma_{z,t-1}^2)$ shown earlier, a larger steady state value for σ_z^2 is implied. The comparative statics with respect to σ_x^2 , σ_ϵ^2 , and σ_μ^2 are analogous.

It is worth noting that $z_{i,t}$ is obtained via Bayesian updating, using the prior belief $\mu_{1,t}^i$ and $y_t - x_{1,t}^i$ shown in Equation (B9). As the variance of the posterior belief is always smaller than the variance of both prior beliefs, we can obtain:

$$0 \leq \sigma_z^2 \leq \min\{\text{Var}^C, \text{Var}^T\}.$$

In a special case when the variance of private signals go to infinity (i.e., $\sigma_e^2 \rightarrow +\infty$, $\sigma_\epsilon^2 \rightarrow +\infty$), the steady state σ_z^2 is:

$$\sigma_z^2 = \frac{-(1-\rho^2)\sigma_\mu^2 + \sqrt{\sigma_\mu^2(1-\rho)^2[(1+\rho)^2\sigma_\mu^2 + 4\sigma_x^2]}}{2(1-\rho)^2}$$

Similarly, considering the case that when the persistence of the cyclical component ρ changes:

$$\frac{\partial \sigma_{z,t}^2}{\partial \rho} = \frac{\sigma_{z,t-1}^2}{g_2(\sigma_{z,t-1}^2)^2} \left\{ 2\sigma_e^4 \sigma_\epsilon^4 [\rho\sigma_\mu^2 + \sigma_x^2] [\sigma_\mu^2 + (1-\rho)\sigma_{z,t-1}^2] \right\} > 0.$$

Therefore, the steady state value of σ_z^2 is increasing in ρ . The logic underlying this statement is analogous.

Proof of Proposition 1. To show the first item, we note the following. When $\sigma_\mu^2 = 0$, according to Lemma 4, σ_z^2 goes to zero, and therefore $\widetilde{\text{COV}}$ becomes zero. When $\sigma_\mu^2 \rightarrow +\infty$, Lemma 4 states that $\sigma_z^2 \rightarrow \min\{\text{Var}^C, \text{Var}^T\}$, but $\Omega \rightarrow +\infty$ in this case. Therefore, $\widetilde{\text{COV}}$ goes to zero.

To show the second term, we first show that the second order derivative of σ_z^2 with respect to σ_μ^2 is negative. In Equation (B12), $g_2(\sigma_{z,t-1}^2)^2$ increases in σ_μ^2 . Then the derivative $\partial \sigma_z^2 / \partial \sigma_\mu^2$ decreases when σ_μ^2 is larger. As σ_μ^2 approaches infinity, $\partial \sigma_z^2 / \partial \sigma_\mu^2$

approaches zero. That is,

$$Z'_\mu \equiv \frac{\partial \sigma_z^2}{\partial \sigma_\mu^2} > 0 \quad \text{and} \quad Z''_\mu \equiv \frac{\partial^2 \sigma_z^2}{(\partial \sigma_\mu^2)^2} < 0.$$

We then derive the derivative with respect to σ_μ^2 :

$$\frac{\partial |\widetilde{\text{COV}}|}{\partial \sigma_\mu^2} \propto Z'_\mu (\sigma_e^2 + \sigma_x^2) (\sigma_\epsilon^2 + \sigma_\mu^2) - \sigma_z^2 (\rho^2 \sigma_z^2 + \sigma_e^2 + \sigma_x^2).$$

We show that evaluated at $\sigma_\mu^2 = 0$,

$$\frac{\partial |\widetilde{\text{COV}}|}{\partial \sigma_\mu^2} \Big|_{\sigma_\mu^2=0} \propto Z'_\mu (\sigma_e^2 + \sigma_x^2) \sigma_\epsilon^2 > 0.$$

That is because $\sigma_z^2 = 0$ when $\sigma_\mu^2 = 0$. The second-order derivative is given by:

$$\frac{\partial^2 |\widetilde{\text{COV}}|}{(\partial \sigma_\mu^2)^2} \propto Z''_\mu (\sigma_\mu^2 + \sigma_\epsilon^2) (\sigma_e^2 + \sigma_x^2) - 2\rho^2 \sigma_z^2 Z'_\mu < 0.$$

To see the inequality we note that $Z'_\mu > 0$, and $Z''_\mu < 0$. Therefore, there exists a unique $\tilde{\sigma}_\mu^2 > 0$, such that $\partial |\widetilde{\text{COV}}| / \partial \sigma_\mu^2 = 0$. For any $\sigma_\mu^2 < \tilde{\sigma}_\mu^2$, $|\widetilde{\text{COV}}|$ is increasing in σ_μ^2 ; and for any $\sigma_\mu^2 > \tilde{\sigma}_\mu^2$, $|\widetilde{\text{COV}}|$ is decreasing in σ_μ^2 . The property that $|\widetilde{\text{COV}}|$ increases and then decrease is implied.

It is straightforward to show the second item that $|\widetilde{\text{COV}}|$ is always increasing in ρ , because

$$\frac{\partial |\widetilde{\text{COV}}|}{\partial \rho} = \frac{\sigma_e^2 \sigma_\epsilon^2}{\Omega^2} \left\{ (\sigma_x^2 + \sigma_e^2) [\sigma_z^4 + \rho Z'_\rho (\sigma_\mu^2 + \sigma_\epsilon^2)] + \sigma_z^2 (\sigma_\mu^2 + \sigma_\epsilon^2) [\sigma_x^2 + \sigma_e^2 - \rho^2 \sigma_z^2] \right\} > 0,$$

where $Z'_\rho \equiv \partial \sigma_z^2 / \partial \rho > 0$.

Proof of Proposition 2. The covariance between the changes in the long term forecasts and the cyclical forecasts is given by:

$$\begin{aligned} COV_F^h &= cov(F_{i,t} y_{t+3Y} - F_{i,t-1} y_{t-1+3Y}, Cyc_{i,t}^h - Cyc_{i,t-1}^h) \\ &= (\rho^h - \rho^{3Y}) \left[cov(\mu_{1,t}^i - \mu_{1,t-1}^i, x_{1,t}^i - x_{1,t-1}^i) + \rho^{3Y} var(x_{1,t}^i - x_{1,t-1}^i) \right] \\ &= (\rho^h - \rho^{3Y}) (\widetilde{\text{COV}} + \rho^{3Y} \text{Var}^C) \\ &= \frac{(\rho^h - \rho^{3Y}) \sigma_e^2}{\Omega} \left\{ \rho^{3Y} [\Omega - \sigma_e^2 (\sigma_\epsilon^2 + \sigma_\mu^2 + \sigma_z^2)] - \rho \sigma_\epsilon^2 \sigma_z^2 \right\} \\ &\propto \rho^{3Y} [\Omega - \sigma_e^2 (\sigma_\epsilon^2 + \sigma_\mu^2 + \sigma_z^2)] - \rho \sigma_\epsilon^2 \sigma_z^2. \end{aligned} \tag{B13}$$

Define $K \equiv \rho^{3Y}[\Omega - \sigma_e^2(\sigma_e^2 + \sigma_\mu^2 + \sigma_z^2)] - \rho\sigma_e^2\sigma_z^2$. Then the sign of the covariance between changes in trend forecasts and changes in cyclical forecasts depends on the sign of K .

To prove the properties in the proposition, we first show that for any given σ_μ^2 , there is a threshold $\bar{\sigma}_x^2$ such that if and only if $\sigma_x^2 < \bar{\sigma}_x^2$, then $K < 0$; and otherwise, $K \geq 0$. To see this, we derive the first-order derivative of K with respect to σ_x^2 :

$$\begin{aligned}\frac{\partial K}{\partial \sigma_x^2} &= \rho^{3Y}[\sigma_z^2 + \sigma_\mu^2 + \sigma_e^2 + \sigma_x^2 Z'_x + \rho^2 Z'_x(\sigma_\mu^2 + \sigma_e^2)] - \rho\sigma_e^2 Z'_x \\ &= Z'_x \left[\rho^{3Y} \left(\frac{\sigma_z^2 + \sigma_\mu^2 + \sigma_e^2}{Z'_x} + \sigma_x^2 + \rho^2\sigma_\mu^2 + \rho^2\sigma_e^2 \right) - \rho\sigma_e^2 \right].\end{aligned}\quad (\text{B14})$$

According to Lemma 4, $Z'_x > 0$ and $Z''_x < 0$. Therefore, the sum of first two terms in Equation (B14), $(\sigma_z^2 + \sigma_\mu^2 + \sigma_e^2)/Z'_x + \sigma_x^2$, increases in σ_x^2 .

If $\partial K/\partial \sigma_x^2 \geq 0$ when evaluated at $\sigma_x^2 = 0$, then it always holds $\partial K/\partial \sigma_x^2 \geq 0$. If $\partial K/\partial \sigma_x^2 < 0$ when evaluated at $\sigma_x^2 = 0$, $\partial K/\partial \sigma_x^2$ crosses zero only once from below. Note that $\partial K/\partial \sigma_x^2$ must be positive when σ_x^2 is sufficiently large.

Furthermore, we characterize how K changes in σ_x^2 . When $\sigma_x^2 = 0$, $K = 0$. That is because $\sigma_z^2 = 0$. When $\sigma_x^2 > 0$, K is either always positive, or K initially decreases and then crosses zero from below. This property implies that for any given value of σ_μ^2 , there exists a threshold $\bar{\sigma}_x^2 \geq 0$, such that $K|_{\sigma_x^2=\bar{\sigma}_x^2} = 0$, and for any $\sigma_x^2 < \bar{\sigma}_x^2$, $K < 0$.

Given this property, we start proving the first item in this proposition. Towards this end, we show the following claim.

Claim: When $\sigma_x^2 = 0$, there exists a threshold $\bar{\sigma}_\mu^2$ for σ_μ^2 , such that when $\sigma_\mu^2 \geq \bar{\sigma}_\mu^2$, $\bar{\sigma}_x^2 = 0$; when $0 < \sigma_\mu^2 < \bar{\sigma}_\mu^2$, $\bar{\sigma}_x^2 > 0$; and when $\sigma_\mu^2 = 0$, $\bar{\sigma}_x^2 = 0$.

To prove this claim, we first evaluate $\partial K/\partial \sigma_x^2$ at $\sigma_x^2 = 0$:

$$\frac{\partial K}{\partial \sigma_x^2}|_{\sigma_x^2=0} = Z'_{x=0} \left[\rho^{3Y} \left(\frac{\sigma_\mu^2 + \sigma_e^2}{Z'_{x=0}} + \rho^2\sigma_\mu^2 + \rho^2\sigma_e^2 \right) - \rho\sigma_e^2 \right],$$

where $Z'_{x=0}$ is derivative of σ_z^2 evaluated at $\sigma_x^2 = 0$. It is given by:

$$Z'_{x=0} \equiv \frac{\partial \sigma_z^2}{\partial \sigma_x^2}|_{\sigma_x^2=0} = \begin{cases} \frac{2\rho(\sigma_e^2 + \sigma_\epsilon^2)}{(1-\rho)(1+\rho)}\sigma_\mu^2 + \frac{2\sigma_e^2\sigma_\epsilon^2}{1+\rho}, & \text{if } \sigma_\mu^2 > 0. \\ 0, & \text{if } \sigma_\mu^2 = 0. \end{cases} \quad (\text{B15})$$

There are only two cases. (i) When $\partial K/\partial \sigma_x^2|_{\sigma_x^2=0} \geq 0$, then K is always positive when $\sigma_x^2 > 0$ and $\bar{\sigma}_x^2 = 0$; and (ii) when $\partial K/\partial \sigma_x^2|_{\sigma_x^2=0} < 0$, K is negative and then crosses zero from below at $\sigma_x^2 = \bar{\sigma}_x^2 > 0$. Therefore, the necessary and sufficient condi-

tion for $\bar{\sigma}_x^2 > 0$ is given by $\partial K / \partial \sigma_x^2|_{\sigma_x^2=0} < 0$, which is equivalent to

$$\rho^{3Y} \left(\frac{\sigma_\mu^2 + \sigma_\epsilon^2}{Z'_{x=0}} + \rho^2 \sigma_\mu^2 + \rho^2 \sigma_\epsilon^2 \right) - \rho \sigma_\epsilon^2 < 0$$

or using the expression of $Z'_{x=0}$ in Equation (B15),

$$\frac{2\rho^4(\sigma_e^2 + \sigma_\epsilon^2)}{1 - \rho^2} (\sigma_\mu^2)^2 + \left[1 + \frac{2\rho^2\sigma_e^2\sigma_\epsilon^2}{1 + \rho} (1 + \rho^2 - \rho^{1-3Y}) \right] \sigma_\mu^2 - \left[\rho(\rho^{-h} - 1) \frac{2\sigma_e^2\sigma_\epsilon^2}{1 + \rho} + \rho^{1-3Y} \right] \sigma_\epsilon^2 < 0. \quad (\text{B16})$$

The left-hand-side of Equation (B16) is quadratic in σ_μ^2 , therefore there are two roots. Note that The left-hand-side of Equation (B16) is decreasing and then increasing in σ_μ^2 and it is negative when $\sigma_\mu^2 = 0$. Therefore, there must exist a unique positive root $\bar{\sigma}_\mu^2 > 0$.

Therefore, when $\sigma_\mu^2 \geq \bar{\sigma}_\mu^2$, $\bar{\sigma}_x^2 = 0$, which implies $K > 0$ on condition that $\sigma_x^2 > 0$. The first item in this proposition is shown. When $0 < \sigma_\mu^2 < \bar{\sigma}_\mu^2$, $\bar{\sigma}_x^2 > 0$, which implies $K > 0$ on condition that $\sigma_x^2 > \bar{\sigma}_x^2$. The second item is shown.

In addition, from the third equivalent of Equation (B13), as the forecast horizon h used to construct the cyclical forecast increases, the magnitude of COV_F^h is decreasing. The third item is shown.

Proof of Proposition 3. Given the optimal forecasts characterized by Lemma 3, the forecast variance across all forecasters is given by:

$$\text{Var}(F_{i,t}y_{t+h}) = E[(\mu_{1,t}^i - \bar{E}[\mu_t])^2] + \rho^{2h}E[(x_{1,t}^i - \bar{E}[x_t])^2] + 2\rho^hE[(\mu_{1,t}^i - \bar{E}[\mu_t])E[(x_{1,t}^i - \bar{E}[x_t])]].$$

$\bar{E}[\cdot]$ stands for the mean forecast across all forecasters. To be specific:

$$E[(\mu_{1,t}^i - \bar{E}[\mu_t])^2] = \text{Var}^T - \frac{\sigma_\epsilon^4(\rho^2\sigma_z^2 + \sigma_x^2 + \sigma_e^2)^2}{\Omega^2} - \frac{\rho^2\sigma_\epsilon^4\sigma_z^4}{\Omega^2} - \frac{\sigma_\epsilon^4(\sigma_e^2 + \sigma_x^2)^2}{\Omega^2} = \text{Var}^T \phi^T,$$

where ϕ^T is given by:

$$\begin{aligned} \phi^T &= 1 - \frac{\sigma_\epsilon^4}{\text{Var}^T} \times \frac{\sigma_\mu^2(\rho^2\sigma_z^2 + \sigma_x^2 + \sigma_e^2)^2 + \rho^2\sigma_x^2\sigma_z^4 + (\sigma_e^2 + \sigma_x^2)^2W\sigma_z^2}{\Omega^2} \\ &= \frac{[V + \sigma_e^2(\sigma_\mu^2 + \sigma_z^2)]^2 + \rho^2\sigma_e^2\sigma_\epsilon^2\sigma_z^4 + \sigma_\epsilon^2(\sigma_e^2 + \sigma_x^2)^2W\sigma_z^2}{\Omega[\Omega - \sigma_\epsilon^2(\sigma_x^2 + \sigma_e^2 + \rho^2\sigma_z^2)]} < 1. \end{aligned}$$

Note that $W = E[(z_{i,t-1} - \bar{E}[z_{i,t-1}])^2]/\sigma_z^2$ is a positive scalar in steady state and invari-

ant in t . To obtain the numerator term $E[(z_{i,t} - \bar{E}[z_{i,t}])^2]$, we rewrite Equation (10) and express $z_{i,t}$ as the follows:

$$\begin{aligned} z_{i,t} &= \frac{\sigma_e^2 \sigma_\epsilon^2}{\Omega(\text{Var}^T + 2\widetilde{\text{COV}} + \text{Var}^C)} \{ -[\sigma_x^2 + \rho(\rho-1)\sigma_z^2]\gamma_t^\mu + [\sigma_\mu^2 + (1-\rho)\sigma_z^2]\gamma_t^x \quad (\text{B17}) \\ &\quad + \sigma_e^2 V \epsilon_{i,t} - \sigma_\epsilon^2 V e_{i,t} + (\rho\sigma_\mu^2 + \sigma_x^2)z_{i,t-1} \}. \end{aligned}$$

This allows us to obtain:

$$z_{i,t} - \bar{E}[z_{i,t}] = \frac{\sigma_e^2 \sigma_\epsilon^2}{\Omega(\text{Var}^T + 2\widetilde{\text{COV}} + \text{Var}^C)} \left[\sigma_e^2 V \epsilon_{i,t} - \sigma_\epsilon^2 V e_{i,t} + (\rho\sigma_\mu^2 + \sigma_x^2)(z_{i,t-1} - \bar{E}[z_{i,t-1}]) \right].$$

and

$$E[(z_{i,t} - \bar{E}[z_{i,t}])^2] = \frac{(\sigma_e^2 + \sigma_\epsilon^2)\sigma_z^2 V^2}{(\sigma_e^2 + \sigma_\epsilon^2)V^2 + \sigma_e^2 \sigma_\epsilon^2 \{ \sigma_\mu^2 [\sigma_x^2 + \rho\sigma_z^2(\rho-1)]^2 + \sigma_x^2 [\sigma_\mu^2 + (1-\rho)\sigma_z^2]^2 \}}.$$

Therefore, W is given by:

$$W = \frac{(\sigma_e^2 + \sigma_\epsilon^2)V^2}{(\sigma_e^2 + \sigma_\epsilon^2)V^2 + \sigma_e^2 \sigma_\epsilon^2 \{ \sigma_\mu^2 [\sigma_x^2 + \rho\sigma_z^2(\rho-1)]^2 + \sigma_x^2 [\sigma_\mu^2 + (1-\rho)\sigma_z^2]^2 \}} < 1.$$

Similarly, $E[(x_{1,t}^i - \bar{E}[x_t])^2]$ and $E[(\mu_{1,t}^i - \bar{E}[\mu_t])]E[(x_{1,t}^i - \bar{E}[x_t])]$ can be written as:

$$E[(x_{1,t}^i - \bar{E}[x_t])^2] = \frac{[V + \sigma_e^2(\sigma_x^2 + \rho^2\sigma_z^2)]^2 + \rho^2\sigma_e^2\sigma_\epsilon^2\sigma_z^4 + \rho^2\sigma_e^2(\sigma_\epsilon^2 + \sigma_\mu^2)^2 W \sigma_z^2}{\Omega[\Omega - \sigma_e^2(\sigma_\epsilon^2 + \sigma_\mu^2 + \sigma_z^2)]} \text{Var}^C = \phi^C \text{Var}^C,$$

and

$$\begin{aligned} E[(\mu_{1,t}^i - \bar{E}[\mu_t])]E[(x_{1,t}^i - \bar{E}[x_t])] \\ = \frac{\sigma_e^2[V + \sigma_e^2(\sigma_x^2 + \rho^2\sigma_z^2)] + \sigma_e^2[V + \sigma_e^2(\sigma_z^2 + \sigma_\mu^2)] + \sigma_e^2\sigma_\epsilon^2(\sigma_x^2 + \sigma_\mu^2)(\sigma_\epsilon^2 + \sigma_\mu^2)W\sigma_z^2}{\Omega\sigma_e^2\sigma_\epsilon^2} \widetilde{\text{COV}} \\ = \phi^{COV} \widetilde{\text{COV}}. \end{aligned}$$

Therefore, the forecast variance of $F_{i,t}y_{t+h}$ across all forecasters can be written as:

$$\text{Var}(F_{i,t}y_{t+h}) = E[(F_{i,t}y_{t+h} - \bar{E}[F_{i,t}y_{t+h}])^2] = \rho^{2h} \text{Var}^C \phi^C + \text{Var}^T \phi^T + 2\rho^h \widetilde{\text{COV}} \phi^{COV},$$

Take the derivative with respect to the forecast horizon h :

$$\frac{\partial \text{Var}(F_{i,t}y_{t+h})}{\partial h} = 2\rho^h \ln \rho (\rho^h \text{Var}^C \phi^C + \widetilde{\text{COV}} \phi^{COV}).$$

The forecast variance is increasing in h if and only if $\partial \text{Var}(F_{i,t}y_{t+h})/\partial h > 0$. That is,

$$h > \underline{h} = \frac{1}{\ln \rho} \ln \frac{-\widetilde{\text{COV}}\phi^{\text{COV}}}{\text{Var}^C\phi^C}.$$

Proof of Proposition 4. Given the beliefs regarding the trend and cyclical components specified in Equations (B1) and (B2), the now-cast error in period t is given by:

$$\begin{aligned} FE_{i,t} &= y_t - F_{i,t}y_t \\ &= \frac{\rho\sigma_e^2\sigma_z^2 + \sigma_e^2(\sigma_x^2 + \sigma_e^2 + \rho^2\sigma_z^2)}{\Omega} \gamma_t^\mu + \frac{\rho\sigma_e^2\sigma_z^2 + \sigma_e^2(\sigma_\mu^2 + \sigma_e^2 + \sigma_z^2)}{\Omega} \gamma_t^x \\ &\quad - \frac{V + \sigma_e^2[(1 - \rho)\sigma_z^2 + \sigma_\mu^2]}{\Omega} \epsilon_{i,t} - \frac{V + \sigma_e^2[\sigma_x^2 + (\rho^2 - \rho)\sigma_z^2]}{\Omega} e_{i,t} \\ &\quad + \frac{\rho\sigma_e^2(\sigma_e^2 + \sigma_\mu^2) - \sigma_e^2(\sigma_e^2 + \sigma_x^2)}{\Omega} z_{i,t-1}. \end{aligned}$$

Since the state innovations and the signal noises (γ_t^μ , γ_t^x , $\epsilon_{i,t}$, $e_{i,t}$) are independent across periods, the correlation between the now-cast errors across periods is:

$$\text{cov}(FE_{i,t-1}, FE_{i,t}) = \frac{\rho\sigma_e^2(\sigma_e^2 + \sigma_\mu^2) - \sigma_e^2(\sigma_e^2 + \sigma_x^2)}{\Omega} \text{cov}(FE_{i,t-1}, z_{i,t-1}).$$

We first examine the correlation between the now-cast error at period $t - 1$ (i.e., $FE_{i,t-1}$) and the separation error at the end of $t - 1$ (i.e., $z_{i,t-1}$).

To begin with, we first demonstrate that in the rational case where $m_1 = m_2 = 1$, the covariance between the now-cast error in period $t - 1$ and the separation error $z_{i,t-1}$ is zero. The now-cast error in period $t - 1$ is given by:

$$\begin{aligned} FE_{i,t-1} &= y_{t-1} - F_{i,t-1}y_{t-1} \\ &= (\mu_{t-1} - \mu_{1,t-1}^i) + (x_{t-1} - x_{1,t-1}^i). \end{aligned}$$

The separation error $z_{i,t-1}$ is given by:

$$z_{i,t-1} = \frac{(\text{Var}^T + \widetilde{\text{COV}})(x_{t-1} - x_{1,t-1}^i) - (\text{Var}^C + \widetilde{\text{COV}})(\mu_{t-1} - \mu_{1,t-1}^i)}{\text{Var}^T + \text{Var}^C + 2\widetilde{\text{COV}}}.$$

Therefore, the covariance is:

$$\text{cov}(FE_{i,t-1}, z_{i,t-1}) = \frac{[(\text{Var}^T + \widetilde{\text{COV}})(\widetilde{\text{COV}} + \text{Var}^C) - (\text{Var}^C + \widetilde{\text{COV}})(\text{Var}^T + \widetilde{\text{COV}})]}{\text{Var}^T + \text{Var}^C + 2\widetilde{\text{COV}}} = 0.$$

Therefore, when $m_1 = m_2 = 1$, the now-cast error in the period $t - 1$ is independent with the separation error $z_{i,t-1}$. Consequently, the now-cast errors across periods $t - 1$ and t would also be zero.

When forecasters are overconfident in the trend signal, i.e., $m_1 < 1, m_2 = 1$. The posterior beliefs regarding the two components after observing the new signals can be written as:

$$\mu_{1,t,o}^T = \frac{m_1\sigma_e^2(\rho^2\sigma_{z,o}^2 + \sigma_x^2 + \sigma_e^2)}{\Omega_1}\mu_{2,t-1,o}^i + \frac{V_1 + \sigma_e^2(\sigma_{z,o}^2 + \sigma_\mu^2)}{\Omega_1}s_{i,t}^\mu - \frac{\rho m_1\sigma_e^2\sigma_{z,o}^2}{\Omega_1}(s_{i,t}^x - \rho x_{2,t-1,o}^i), \quad (\text{B18})$$

$$x_{1,t,o}^T = \frac{\sigma_e^2(\sigma_{z,o}^2 + \sigma_\mu^2 + m_1\sigma_e^2)}{\Omega_1}\rho x_{2,t-1,o}^i + \frac{V_1 + m_1\sigma_e^2(\sigma_x^2 + \rho^2\sigma_{z,o}^2)}{\Omega_1}s_{i,t}^x - \frac{\rho\sigma_e^2\sigma_{z,o}^2}{\Omega_1}(s_{i,t}^\mu - \mu_{2,t-1,o}^i), \quad (\text{B19})$$

where Ω_1 and V_1 are constants:

$$\Omega_1 = (\sigma_{z,o}^2 + \sigma_\mu^2 + m_1\sigma_e^2)(\sigma_x^2 + \sigma_e^2 + \rho^2\sigma_{z,o}^2) - \rho^2\sigma_{z,o}^4, \quad V_1 = (\sigma_{z,o}^2 + \sigma_\mu^2)(\sigma_x^2 + \rho^2\sigma_{z,o}^2) - \rho^2\sigma_{z,o}^4.$$

The term $\sigma_{z,o}^2$ is the perceived variance of the separation error in the steady state in this case. The variance-covariance matrix regarding the beliefs of the trend and cyclical components is:

$$\begin{pmatrix} \text{Var}_1^T & \widetilde{\text{COV}}_1 \\ \widetilde{\text{COV}}_1 & \text{Var}_1^C \end{pmatrix} = \begin{pmatrix} \frac{m_1\sigma_e^2[\Omega_1 - m_1\sigma_e^2(\sigma_x^2 + \sigma_e^2 + \rho^2\sigma_{z,o}^2)]}{\Omega_1} & -\frac{\rho\sigma_e^2m_1\sigma_e^2\sigma_{z,o}^2}{\Omega_1} \\ -\frac{\rho\sigma_e^2m_1\sigma_e^2\sigma_{z,o}^2}{\Omega_1} & \frac{\sigma_e^2[\Omega_1 - \sigma_e^2(m_1\sigma_e^2 + \sigma_\mu^2 + \sigma_{z,o}^2)]}{\Omega_1} \end{pmatrix}. \quad (\text{B20})$$

Importantly, the perceived variances of both the trend and cyclical components, as well as their covariance (in magnitude), are lower:

$$\text{Var}_a^T = \text{Var}_1^T + (1 - m_1)\sigma_e^2\left(\frac{V_1 + \sigma_e^2(\sigma_{z,o}^2 + \sigma_\mu^2)}{\Omega_1}\right)^2 + \left(\frac{m_1\sigma_e^2(\sigma_x^2 + \sigma_e^2)}{\Omega_1}\right)^2(\sigma_{z,a}^2 - \sigma_{z,o}^2), \quad (\text{B21})$$

$$\text{Var}_a^C = \text{Var}_1^C + (1 - m_1)\sigma_e^2\left(\frac{\rho\sigma_e^2\sigma_{z,o}^2}{\Omega_1}\right)^2 + \left(\frac{\rho\sigma_e^2(\sigma_\mu^2 + m_1\sigma_e^2)}{\Omega_1}\right)^2(\sigma_{z,a}^2 - \sigma_{z,o}^2), \quad (\text{B22})$$

$$\begin{aligned} \widetilde{\text{COV}}_a &= \widetilde{\text{COV}}_1 - (1 - m_1)\sigma_e^2\frac{\rho\sigma_e^2\sigma_{z,o}^2}{\Omega_0}\frac{V_1 + \sigma_e^2(\sigma_{z,o}^2 + \sigma_\mu^2)}{\Omega_1} \\ &\quad - \frac{m_1\sigma_e^2(\sigma_x^2 + \sigma_e^2)}{\Omega_1}\frac{\rho\sigma_e^2(\sigma_\mu^2 + m_1\sigma_e^2)}{\Omega_1}(\sigma_{z,a}^2 - \sigma_{z,o}^2). \end{aligned} \quad (\text{B23})$$

The subscript a stands for the actual variance and covariance term when forecasters

are overconfident in the trend signal. $\sigma_{z,a}^2$ is the actual variance of the separation error:

$$\sigma_{z,a}^2 - \sigma_{z,o}^2 = G^T(1 - m_1)\sigma_\epsilon^2\left(\frac{\sigma_e^2 V_1}{\Omega_1}\right)^2 > 0,$$

where G^T is given by:

$$G^T = \frac{\Omega_1^2}{[\Omega_1(\text{Var}_1^T + \text{Var}_1^C + 2\widetilde{\text{COV}}_1)]^2 - [m_1\sigma_e^2\sigma_\epsilon^2(\rho\sigma_\mu^2 + \sigma_x^2)]^2} > 0.$$

At the end of period $t-1$, when the actual state value y_{t-1} is observed by all the forecasters, they will revise their beliefs using the perceived variance-covariance matrix. The separation error $z_{i,t-1}$ in this case can be written as:

$$z_{i,t-1,o} = \frac{(\text{Var}_1^T + \widetilde{\text{COV}}_1)(x_{t-1} - x_{1,t-1,o}^T) - (\text{Var}_1^C + \widetilde{\text{COV}}_1)(\mu_{t-1} - \mu_{1,t-1,o}^T)}{\text{Var}_1^T + \text{Var}_1^C + 2\widetilde{\text{COV}}_1}.$$

The covariance between $FE_{i,t-1}$ and $z_{i,t-1,o}$ is given by:

$$\begin{aligned} & \text{cov}(FE_{i,t-1}, z_{i,t-1,o}) \\ &= (\text{Var}_1^T + \widetilde{\text{COV}}_1)(\text{Var}_a^C + \widetilde{\text{COV}}_a) - (\text{Var}_1^C + \widetilde{\text{COV}}_1)(\text{Var}_a^T + \widetilde{\text{COV}}_a) \\ &= (\text{Var}_1^T + \widetilde{\text{COV}}_1)(\text{Var}_a^C - \text{Var}_1^C + \widetilde{\text{COV}}_a - \widetilde{\text{COV}}_1) \\ &\quad - (\text{Var}_1^C + \widetilde{\text{COV}}_1)(\text{Var}_a^T - \text{Var}_1^T + \widetilde{\text{COV}}_a - \widetilde{\text{COV}}_1). \end{aligned} \tag{B24}$$

The second equality in Equation (B24) holds because we subtract the following term to the right-hand-side:

$$(\text{Var}_1^T + \widetilde{\text{COV}}_1)(\text{Var}_1^C + \widetilde{\text{COV}}_1) - (\text{Var}_1^C + \widetilde{\text{COV}}_1)(\text{Var}_1^T + \widetilde{\text{COV}}_1) = 0. \tag{B25}$$

This term is zero because it is the perceived covariance $FE_{i,t-1}$ and $z_{i,t-1}$. Using Equations (B21) to (B24), we have:

$$\text{cov}(FE_{i,t-1}, z_{i,t-1,o}) = -(1 - m_1)\sigma_\epsilon^2\phi_{over}^T\frac{\sigma_e^2 V_1}{\Omega_1}, \tag{B26}$$

where

$$\begin{aligned} \phi_{over}^T &= \frac{1}{\Omega_1^3}[(1 - \rho)\sigma_e^2(\sigma_\mu^2 + \sigma_{z,o}^2 + m_1\sigma_e^2) + V_1 + m_1\sigma_e^2\sigma_x^2][m_1\sigma_e^4\sigma_\epsilon^2 V_1(\rho\sigma_\mu^2 + \sigma_x^2)]G^T \\ &\quad + \frac{V_1 + \sigma_e^2[\sigma_\mu^2 + (1 - \rho)\sigma_{z,o}^2]}{\Omega_1}[1 - \frac{G^T}{\Omega_1^2}m_1\sigma_e^4\sigma_\epsilon^2 V_1(\rho\sigma_\mu^2 + \sigma_x^2)] > 0. \end{aligned}$$

Therefore, when forecasters exhibit overconfidence in the trend signal, there is always a negative correlation between the now-cast error $FE_{i,t-1}$ and the separation error $z_{i,t-1,o}$. Consequently, the covariance between the now-cast errors across periods can be expressed as:

$$cov(FE_{i,t-1}, FE_{i,t}) = \frac{\rho\sigma_e^2(m_1\sigma_e^2 + \sigma_\mu^2) - m_1\sigma_e^2(\sigma_e^2 + \sigma_x^2)}{\Omega_1} \underbrace{cov(FE_{i,t-1}, z_{i,t-1})}_{(-)}.$$

The condition for a positive correlation between the now-cast errors across periods then in given by:

$$\frac{\rho\sigma_e^2(m_1\sigma_e^2 + \sigma_\mu^2) - m_1\sigma_e^2(\sigma_e^2 + \sigma_x^2)}{\Omega_1} < 0,$$

which is equivalent to

$$\frac{\rho\sigma_\mu^2\sigma_e^2}{\sigma_e^2[(1-\rho)\sigma_e^2 + \sigma_x^2]} < m_1 < 1.$$

Following the same logic, when forecasters are overconfident in the cyclical signal, the variance-covariance matrix of regarding the beliefs of the trend and cyclical components is:

$$\begin{pmatrix} \text{Var}_2^T & \widetilde{\text{COV}}_2 \\ \widetilde{\text{COV}}_2 & \text{Var}_2^C \end{pmatrix} = \begin{pmatrix} \frac{\sigma_e^2[\Omega_2 - \sigma_e^2(\sigma_x^2 + m_2\sigma_e^2 + \rho^2\sigma_{z,o}^2)]}{\Omega_2} & -\frac{\rho m_2\sigma_e^2\sigma_\epsilon^2\sigma_{z,o}^2}{\Omega_2} \\ -\frac{\rho m_2\sigma_e^2\sigma_\epsilon^2\sigma_{z,o}^2}{\Omega_2} & \frac{m_2\sigma_e^2[\Omega_2 - m_2\sigma_e^2(\sigma_e^2 + \sigma_\mu^2 + \sigma_{z,o}^2)]}{\Omega_2} \end{pmatrix}. \quad (\text{B27})$$

The covariance between the now-cast error at $t-1$ and the separation error $z_{i,t-1,o}$ is given by:

$$cov(FE_{i,t-1}, z_{i,t-1,o}) = (1-m_2)\sigma_e^2\phi_{over}^C \frac{\sigma_e^2 V_2}{\Omega_2}, \quad (\text{B28})$$

where Ω_2 and V_2 are counterparts of Ω_1 and V_1 :

$$\Omega_2 = (\sigma_{z,o}^2 + \sigma_\mu^2 + \sigma_e^2)(\sigma_x^2 + m_2\sigma_e^2 + \rho^2\sigma_{z,o}^2) - \rho^2\sigma_{z,o}^4, \quad V_2 = (\sigma_{z,o}^2 + \sigma_\mu^2)(\sigma_x^2 + \rho^2\sigma_{z,o}^2) - \rho^2\sigma_{z,o}^4.$$

and

$$\begin{aligned} \phi_{over}^C &= \frac{\sigma_e^2[\sigma_x^2 - \rho(1-\rho)\sigma_{z,o}^2] + V_2}{\Omega_2}[1 - \rho G^C \frac{m_2\sigma_e^4\sigma_\epsilon^2 V_2(\sigma_\mu^2 + \sigma_x^2)}{\Omega_2^2}] \\ &+ \frac{1}{\Omega_2^3}[V_2 + m_1\sigma_e^2(\sigma_\mu^2 + (1-\rho)\sigma_x^2)][m_2\sigma_e^4\sigma_\epsilon^2 V_2(\sigma_\mu^2 + \sigma_x^2)]G^C > 0. \end{aligned}$$

G^C is the counterpart of G^T :

$$G^C = \frac{\Omega_2^2}{[\Omega_2(\text{Var}_2^T + \text{Var}_2^C + 2\widetilde{\text{COV}}_2)]^2 - [m_2\sigma_e^2\sigma_\epsilon^2(\rho\sigma_\mu^2 + \sigma_x^2)]^2} > 0.$$

Equation (B28) shows that when forecasters are overconfident in the cyclical signal, the correlation between the now-cast error at $t - 1$ and the separation error $z_{i,t-1,o}$ would be positive. The covariance between the now-cast errors across periods is given by:

$$\text{cov}(FE_{i,t-1}, FE_{i,t}) = \frac{\rho m_2 \sigma_e^2 (\sigma_e^2 + \sigma_\mu^2) - \sigma_e^2 (m_2 \sigma_e^2 + \sigma_x^2)}{\Omega_2} \underbrace{\text{cov}(FE_{i,t-1}, z_{i,t-1})}_{(+)}.$$

Thus, the now-cast errors are positively correlated across periods if and only if:

$$1 < \frac{1}{m_2} < \frac{1}{\underline{m}_2} = \frac{\sigma_e^2 [\rho \sigma_\mu^2 - (1 - \rho) \sigma_e^2]}{\sigma_e^2 \sigma_x^2}.$$

C Supplemental materials

C.1 Common Shock

In this section, we analyze the case of correlated trend and cyclical components driven by a common shock, by following Delle Monache et al. (2024). They show the presence of a common shock influencing both the trend and cyclical components of GDP growth in the same direction.

This common shock assumption is widely used in the literature. It captures situations where economic shocks have both transitory and permanent effects. Many studies show that recessions impact the economy in both temporary and lasting ways. For example, Furlanetto et al. (2025) and Antolin-Diaz et al. (2017) show that supply shocks can negatively affect both the cyclical and permanent components of GDP. Similarly, Almeida et al. (2004) finds that an increase in firms' profitability can permanently elevate their cash flows while also boosting short-term cash flows by reducing potential losses.

In this section, we consider the following state generation process:

$$\begin{aligned} y_t &= \mu_t + x_t, \\ \mu_t &= \mu_{t-1} + \gamma_t^\mu + \delta_t \quad \text{and} \quad x_t = \rho x_{t-1} + \gamma_t^x + b\delta_t, \end{aligned}$$

where δ_t is a common shock affecting both the trend and cyclical components. This shock is normally distributed with zero mean and variance σ_δ^2 , and is independent across periods (i.e., $\delta_t \sim N(0, \sigma_\delta^2)$). The scalar b measures the relative importance of the shock to each of these components. Notably, following Delle Monache et al. (2024), we assume that b is positive, thereby capturing the common shock assumption.

To contrast with our benchmark model, we assume in this case that the trend component becomes observable at the end of each period. With the information structure,

the belief updating process is given by:

$$\theta_{1,t}^i = \theta_{2,t-1}^i + \kappa_{cor}(s_{i,t} - \theta_{2,t-1}^i), \quad (C1)$$

where $\theta_{2,t-1}^i = (\mu_{t-1}, \rho x_{t-1})'$. Since forecasters are able to observe the actual trend and cyclical components at the end of each period, κ_{cor} is the corresponding Kalman gain matrix given by:

$$\kappa_{cor} = \begin{pmatrix} \frac{\tau_2^\mu}{\tau_1^\mu + \tau_2^\mu + \tau_3^\mu} & \frac{\tau_3^\mu}{b(\tau_1^\mu + \tau_2^\mu + \tau_3^\mu)} \\ \frac{b\tau_3^x}{\tau_1^x + \tau_2^x + \tau_3^x} & \frac{\tau_2^x}{\tau_1^x + \tau_2^x + \tau_3^x} \end{pmatrix}, \quad (C2)$$

where $\tau_1^\mu, \tau_2^\mu, \tau_3^\mu, \tau_1^x, \tau_2^x, \tau_3^x$ are the precisions of information:

$$\begin{aligned} \tau_1^\mu &= \frac{1}{\sigma_\mu^2 + \sigma_\delta^2}; & \tau_2^\mu &= \frac{1}{\sigma_\epsilon^2}; & \tau_3^\mu &= \frac{b^2}{b^2\sigma_\mu^2 + \sigma_x^2 + \sigma_\epsilon^2}; \\ \tau_1^x &= \frac{1}{\sigma_x^2 + b^2\sigma_\delta^2}; & \tau_2^x &= \frac{1}{\sigma_\epsilon^2}; & \tau_3^x &= \frac{1}{b^2\sigma_\mu^2 + b^2\sigma_\epsilon^2 + \sigma_x^2}. \end{aligned}$$

As shown in Equation (C2), the elements on the sub-diagonal is non-zero if $b \neq 0$. Given $b > 0$, the sub-diagonal elements are positive. This is because the surprise from the trend signal (i.e., $s_{i,t}^\mu - \mu_{t-1}$) contains information about the common shock, which also affects the cyclical components. Therefore, forecasters would use the trend signal to update their belief about the cyclical belief, and vice versa.

We show that in this case, the covariance between forecasters' trend beliefs and cyclical beliefs (i.e., $\widetilde{\text{COV}}_{cor}$) is always positive:

$$\widetilde{\text{COV}}_{cor} \propto b(\sigma_\delta^2 + \sigma_\mu^2)[b^2(\sigma_\epsilon^2 + \sigma_\mu^2) + \sigma_\epsilon^2 + \sigma_x^2][\sigma_\delta^2(b^2\sigma_\epsilon^2 + b^2\sigma_\mu^2 + \sigma_\epsilon^2 + \sigma_x^2) + \sigma_\epsilon^2(\sigma_\epsilon^2 + \sigma_\mu^2) + \sigma_\epsilon^2\sigma_x^2]. \quad (C3)$$

With a positive covariance, predictions of this particular case would be similar to the special case discussed in Section 4.1, and therefore inconsistent with the observed empirical pattern.

C.2 Overconfident in cyclical signal

When forecasters are overconfident in the cyclical signal, they perceive the precision of the cyclical signal to be higher than it actually is. Consequently, the error term in the cyclical belief is assigned an excessive weight compared to the Bayesian scenario. As a result, it drives the correlation between the separating error ($z_{i,t-1}$) and the now-cast error for the previous period ($FE_{i,t-1}$) to become positive. Specifically, we show that the covariance is given by:

$$\text{cov}(z_{i,t-1}, FE_{i,t-1}) = (1 - m_2)\sigma_e\phi_O^C \frac{\sigma_\epsilon^2 V_2}{\Omega_2} > 0,$$

where ϕ_O^C is a positive scalar shown in the proof of Proposition 4.

Similar to the case in the main text, when forecasters are overconfident in the cyclical signal, the covariance between the separation error and the now-cast error of the current period can also be decomposed into two parts:

$$\text{cov}(z_{i,t-1}, FE_{i,t}) = \frac{\sigma_z^2}{\Omega_2} \underbrace{[-\sigma_e^2(\sigma_x^2 + m_2\sigma_e^2)]}_{\text{trend prior effect}} + \underbrace{\rho m_2\sigma_e^2(\sigma_\mu^2 + \sigma_e^2)}_{\text{cyclical prior effect}}. \quad (\text{C4})$$

When forecasters are overconfident in the cyclical signal, they tend to place greater reliance on the cyclical signal and less on the prior belief inherited from the last period. Therefore, as the extent of overconfidence in the cyclical signal increases (i.e., m_2 becomes smaller), the effect of the cyclical prior is more likely to be dominated, and the covariance between the separation error ($z_{i,t-1}$) and the current now-cast error ($FE_{i,t}$) is more likely to be negative. Consider a polar case where m_2 goes to zero, the covariance is strictly negative.

Part (ii) of Proposition 4 states that when both the confusion and overconfidence mechanisms are present, the now-cast errors across periods can be positively correlated if the extent of overconfidence in the cyclical signal is moderate. The inequality in Equation (20) characterizes the condition under which the effect of the cyclical prior dominates the effect of the trend prior. Consider the case when the trend component is very volatile (i.e., σ_μ^2 is large enough). Forecasters would place limited reliance on the trend prior and rely heavily on the signal regarding the trend component. Therefore, the effect of the trend prior is always dominated, resulting in a positive correlation between the separation error and the now-cast error of the current period. Consequently, the covariance between the now-cast errors across periods is positive for any $m_2 < 1$.

C.3 Forecast of other forecasters

This section characterizes the case where forecasters not only observe the actual state value but also observe the forecasts from other forecasters. In our model, the individual forecast error comprises both the individual-specific forecast error and the common forecast error, while the consensus forecast includes only the common forecast error. Therefore, forecaster i would anchor to the consensus forecasts after observing the entire distribution.

That is, at the end of the period $t-1$, the individual separation error $z_{i,t-1}$ would be the same across different forecasters (i.e., $z_{t-1} = z_{i,t-1} = z_{j,t-1}$ for any i, j). Specifically, at the end of period t , forecasters observe the actual state value of the current period, y_{t-1} , and the forecasts, $F_{i,t-1}y_{t-1+h}$, from other forecasters. The separation error, z_{t-1} ,

is given by:

$$z_{t-1} = \frac{(\bar{\text{Var}}^T + \bar{\text{COV}})(x_{t-1} - x_{1,t-1}) - (\bar{\text{Var}}^C + \bar{\text{COV}})(\mu_{t-1} - \mu_{1,t-1})}{(\bar{\text{Var}}^T + \bar{\text{COV}}) + (\bar{\text{Var}}^C + \bar{\text{COV}})} \neq 0,$$

where $\mu_{t-1} - \mu_{1,t-1}$ and $x_{t-1} - x_{1,t-1}$ are the consensus forecast errors regarding the trend component and cyclical component:

$$\begin{aligned} \mu_{t-1} - \mu_{1,t-1} &= \frac{\sigma_e^2(\rho^2\bar{\sigma}_z^2 + \sigma_x^2 + \sigma_e^2)}{\bar{\Omega}}\gamma_{t-1}^\mu + \frac{\rho\sigma_e^2\bar{\sigma}_z^2}{\bar{\Omega}}\gamma_{t-1}^x - \frac{\sigma_e^2(\sigma_x^2 + \sigma_e^2)}{\bar{\Omega}}z_{t-2}, \\ x_{t-1} - x_{1,t-1} &= \frac{\rho\sigma_e^2\bar{\sigma}_z^2}{\bar{\Omega}}\gamma_{t-1}^\mu + \frac{\sigma_e^2(\bar{\sigma}_z^2 + \sigma_\mu^2 + \sigma_e^2)}{\bar{\Omega}}\gamma_{t-1}^x + \frac{\rho\sigma_e^2(\sigma_\mu^2 + \sigma_e^2)}{\bar{\Omega}}z_{t-2}. \end{aligned}$$

At the beginning of the current period t , after observing their private signals, individual forecasters' beliefs regarding the trend and cyclical components are still heterogeneous. Their beliefs are given by:

$$\begin{aligned} \mu_{1,t}^i &= \frac{\sigma_e^2(\rho^2\bar{\sigma}_z^2 + \sigma_x^2 + \sigma_e^2)}{\bar{\Omega}}\mu_{2,t-1} + \frac{\bar{V} + \sigma_e^2(\bar{\sigma}_z^2 + \sigma_\mu^2)}{\bar{\Omega}}s_{i,t}^\mu - \frac{\rho\sigma_e^2\bar{\sigma}_z^2}{\bar{\Omega}}(s_{i,t}^x - \rho x_{2,t-1}), \\ x_{1,t}^i &= \frac{\sigma_e^2(\bar{\sigma}_z^2 + \sigma_\mu^2 + \sigma_e^2)}{\bar{\Omega}}\rho x_{2,t-1} + \frac{\bar{V} + \sigma_e^2(\sigma_x^2 + \rho^2\bar{\sigma}_z^2)}{\bar{\Omega}}s_{i,t}^x - \frac{\rho\sigma_e^2\bar{\sigma}_z^2}{\bar{\Omega}}(s_{i,t}^\mu - \mu_{2,t-1}), \end{aligned}$$

where $\bar{\sigma}_z^2$ is the variance of the common separation error. Note that $\mu_{2,t-1} = \mu_{t-1} + z_{t-1}$ and $\rho x_{2,t-1} = \rho x_{t-1} - \rho z_{t-1}$ are the common prior beliefs. Furthermore, $\bar{\Omega}$ and \bar{V} are constants:

$$\bar{\Omega} = (\bar{\sigma}_z^2 + \sigma_\mu^2 + \sigma_e^2)(\sigma_x^2 + \sigma_e^2 + \rho^2\bar{\sigma}_z^2) - \rho^2\bar{\sigma}_z^4, \quad \bar{V} = (\bar{\sigma}_z^2 + \sigma_\mu^2)(\sigma_x^2 + \rho^2\bar{\sigma}_z^2) - \rho^2\bar{\sigma}_z^4.$$

In summary, if forecasters can observe all the forecasts provided by other forecasters, the separation error across all forecasters would be common, which would be a weighted average of all historical state innovations. However, it is still non-zero, indicating that forecasters still cannot perfectly separate the two components. Therefore, our results obtained under the benchmark model still hold.

C.4 Noisy state Signal

In each period, forecaster i observe a private of the actual state y_t :

$$s_{i,t} = y_t + \epsilon_{i,t}, \quad \text{with } \epsilon_{i,t} \sim N(0, \sigma_\epsilon^2).$$

Without loss of generality, forecaster i 's trend and cyclical beliefs can be written as:

$$F_{i,t}\mu_t = \sum_{k=0}^t \alpha_{1,k}\gamma_k^\mu + \sum_{k=0}^t \alpha_{2,k}\gamma_k^x + \sum_{k=0}^t \alpha_{3,k}\epsilon_{i,k};$$

$$F_{i,t}x_t = \sum_{k=0}^t \beta_{1,k}\gamma_k^\mu + \sum_{k=0}^t \beta_{2,k}\gamma_k^x + \sum_{k=0}^t \beta_{3,k}\epsilon_{i,k},$$

where $\alpha_{1,k}, \alpha_{2,k}, \alpha_{3,k}, \beta_{1,k}, \beta_{2,k}$, and $\beta_{3,k}$ are the weights assigned to the trend, cycle innovation, and signal noise for period k .

The average beliefs regarding the trend and cyclical components are:

$$F_t\mu_t = \sum_{k=0}^t \alpha_{1,k}\gamma_k^\mu + \sum_{k=0}^t \alpha_{2,k}\gamma_k^x; \quad F_tx_t = \sum_{k=0}^t \beta_{1,k}\gamma_k^\mu + \sum_{k=0}^t \beta_{2,k}\gamma_k^x.$$

The forecast dispersion is:

$$E[(F_{i,t}y_{t+h} - F_ty_{t+h})^2] = \sum_{k=0}^t (\alpha_{3,k} + \rho^h \beta_{3,k})^2 \sigma_\epsilon^2. \quad (\text{C5})$$

Therefore, the forecast dispersion increases with the forecast horizon h if and only if $\alpha_{3,k}$ and $\beta_{3,k}$ have opposite signs.

In the following, we consider a special case where the forecasters know the exact historical values of the trend and cyclical components, in other words:

$$F_{i,t-1}\mu_t = \mu_{t-1}; \quad F_{i,t-1}x_t = \rho x_{t-1}.$$

Upon observing the signal $s_{i,t}$, the forecaster's updated beliefs regarding the trend and cycle are:

$$\begin{aligned} F_{i,t}\mu_t &= \frac{\sigma_\mu^2(s_{i,t} - F_{i,t-1}x_t) + (\sigma_x^2 + \sigma_\epsilon^2)F_{i,t-1}\mu_t}{\sigma_\mu^2 + \sigma_x^2 + \sigma_\epsilon^2} \\ &= \mu_t + \frac{1}{\sigma_\mu^2 + \sigma_x^2 + \sigma_\epsilon^2} [\sigma_\mu^2(\gamma_t^x + \epsilon_{i,t}) - (\sigma_x^2 + \sigma_\epsilon^2)\gamma_t^\mu], \end{aligned} \quad (\text{C6})$$

$$\begin{aligned} F_{i,t}x_t &= \frac{\sigma_x^2(s_{i,t} - F_{i,t-1}\mu_t) + (\sigma_\mu^2 + \sigma_\epsilon^2)F_{i,t-1}x_t}{\sigma_\mu^2 + \sigma_x^2 + \sigma_\epsilon^2} \\ &= x_t + \frac{1}{\sigma_\mu^2 + \sigma_x^2 + \sigma_\epsilon^2} [\sigma_x^2(\gamma_t^\mu + \epsilon_{i,t}) - (\sigma_\mu^2 + \sigma_\epsilon^2)\gamma_t^x]. \end{aligned} \quad (\text{C7})$$

In Equations (C6) and (C7), two important features need to be emphasized. First, the

covariance between the trend belief and the cyclical belief is given by $cov(F_{i,t}\mu_t, F_{i,t}x_t) = -\frac{\sigma_\mu^2\sigma_x^2}{\sigma_\mu^2+\sigma_x^2+\sigma_\epsilon^2} < 0$. Given the negative covariance between trend and cyclical beliefs, the covariance between changes in long-run beliefs and cyclical beliefs could also be negative, which is analogous to our base model.

Second, both trend belief and cyclical belief increase with signal noise $\epsilon_{i,t}$. In other words, in Equation (C5), α_3 and β_3 have the same sign, which results in decreasing forecast dispersion as the horizon extends.